Engineering Approaches for Cardiac Organoid formation and their characterization

Binata Joddar, Sylvia L. Natividad-Diaz, Andie E. Padilla, Aibhlin A. Esparza, Salma P. Ramirez, David R. Chambers, Hakima Ibaroudene

PII: S1931-5244(22)00182-7

DOI: https://doi.org/10.1016/j.trsl.2022.08.009

Reference: TRSL 1692

To appear in: Translational Research

Received date: 14 June 2022 Revised date: 5 August 2022 Accepted date: 15 August 2022



Please cite this article as: Binata Joddar, Sylvia L. Natividad-Diaz, Andie E. Padilla, Aibhlin A. Esparza, Salma P. Ramirez, David R. Chambers, Hakima Ibaroudene, Engineering Approaches for Cardiac Organoid formation and their characterization, *Translational Research* (2022), doi: https://doi.org/10.1016/j.trsl.2022.08.009

This is a PDF file of an article that has undergone enhancements after acceptance, such as the addition of a cover page and metadata, and formatting for readability, but it is not yet the definitive version of record. This version will undergo additional copyediting, typesetting and review before it is published in its final form, but we are providing this version to give early visibility of the article. Please note that, during the production process, errors may be discovered which could affect the content, and all legal disclaimers that apply to the journal pertain.

© 2022 Elsevier Inc. All rights reserved.

Engineering Approaches for Cardiac Organoid formation and their characterization

Binata Joddar^{a,b,c}*, Sylvia L. Natividad-Diaz^{b,c}, Andie E. Padilla^{a,b}, Aibhlin A. Esparza^b, Salma P. Ramirez^{a,b}, David R. Chambers^d, Hakima Ibaroudene^d

^aInspired Materials & Stem-Cell Based Tissue Engineering Laboratory (IMSTEL),

^bDepartment of Metallurgical, Materials and Biomedical Engineering, University of Texas at El Paso, El Paso, Texas

^cBorder Biomedical Research Center, University of Texas at El Paso, El Paso, Texas

^dSouthwest Research Institute, San Antonio, Texas

*Corresponding Author

Abstract:

Cardiac organoids are three-dimensional (3D) structures composed of tissue or niche-specific cells, obtained from diverse sources, encapsulated in either a naturally derived or synthetic, extracellular matrix scaffold, and include exogenous biochemical signals such as essential growth factors. The overarching goal of developing cardiac organoid models is to establish a functional integration of cardiomyocytes with physiologically relevant cells, tissues, and structures like capillary-like networks composed of endothelial cells. These organoids used to model human heart anatomy, physiology, and disease pathologies in vitro have the potential to solve many issues related to cardiovascular drug discovery and fundamental research. The advent of patient-specific human-induced pluripotent stem cell (hiPSC)-derived cardiovascular cells provides a unique, single-source approach to study the complex process of cardiovascular disease progression through organoid formation and incorporation into relevant, controlled microenvironments such as microfluidic devices. Strategies that aim to accomplish such a feat include microfluidic technology-based approaches, microphysiological systems, microwells, microarray-based platforms, 3D bioprinted models, and electrospun fiber mat-based scaffolds. This article discusses the engineering or technology-driven practices for making cardiac organoid models in comparison with self-assembled or scaffold-free methods to generate organoids. We further discuss emerging strategies for characterization of the bio-assembled cardiac organoids including electrophysiology and machine-learning and conclude with prospective points of interest for engineering cardiac tissues in vitro.

Abbreviations:

CVD, Cardiovascular Diseases; hiPSC, Human Induced Pluripotent Stem Cell; ECM, Extracellular Matrix; HyA, Hyaluronic Acid; PEG, Polyethylene Glycol; NIPAAM, N-isopropyl Acrylamide; ECs, Endothelial Cells; BECs, Blood Vascular Endothelial Cells; LECs, Lymphatic Endothelial Cells; SLA, Stereolithography; MPSs, Microphysiological Systems; PDMS, Polydimethylsiloxane; EMT Epithelial to Mesenchymal; hMSCs, Human Mesenchymal Stem Cells; ALP, Alkaline Phosphatase; Cx43, Connexin-43; CMs, Cardiomyocytes; CFs, Cardiac Fibroblasts; PGA, Polyglycolide; PLA, Poly(L-lactide); PLGA, Poly(lactide-co-glycolide); PCL, Poly(-caprolactone); PEG, Polyethylene glycol; GelMA, Gelatin Methacryloyl; SEM, Scanning Electron Microscopy; FTIR, Fourier Transformed Infrared; -SMA, Alpha-Smooth Muscle Actin; HUVECs, Human Umbilical Vein Endothelial Cells; VEGF, Vascular Endothelial Growth Factor; bFGF, Basic Fibroblast Growth Factor; TGF- ,Transforming Growth Factor; LV, Left Ventricle;

PGS, Polyglycerol Sebacate; TEM, Transmission Electron Microscopy; EPHYS, Electrophysiology; PPy, Polypyrrole; PEDOT, Poly(3,4- ethylenedioxythiophene); PSS, Polystyrene Sulfonate; MEA, Microelectrode Arrays; hCS, Human Cerebral Cortex; hSpS, Human Hindbrain/cerebral Cortex; GLMs, Generalized Linear Models; RNA, Ribonucleic Acid; RNA-seq, RNA sequencing; GO, Gene Ontology; GSEA, Gene Set Enrichment Analysis; scRNA-seq, Single-Cell RNA Sequencing; DE, Differential Expression.

1. Introduction

Due to the limited availability of human myocardium samples and the difficulty associated with culturing primary cardiomyocytes, cardiovascular tissue and diseases (CVDs) are difficult to study and model in vitro [1-3]. Currently in vivo animal studies are used for fundamental cardiovascular research and to screen novel CVD therapeutics but are inefficient due to the associated high cost and advanced technical skill levels required to perform this work. Additionally, although animal models may resemble human heart structure, previous studies have shown significant differences from human cardiovascular physiology including beat rate, vascular flow rate, biochemical signaling, and gene expression [4-6]. In vitro organoid and tissue-on-a-chip models provide a less expensive, more controlled, and reproducible platform for better quantification of isolated cellular processes in response to a biochemical or biophysical stimulus [6-12]. Cardiac organoids have the potential to solve many issues related to cardiovascular drug discovery and fundamental research because they can model human heart structure, physiology, and disease pathologies in vitro. The cardiac organoids described in this review are three-dimensional (3D) structures composed of niche or tissuespecific cells obtained or derived from many sources including pluripotent stem cells, adult stem cells, and primary or immortalized cell lines. These cells are typically encapsulated in a naturally-derived or synthetic extracellular matrix which may contain exogenously added biochemical signals to form the complete organoid. The Organ/Tissue-on-a-Chip model is then developed by incorporating the organoids in a dynamic culture platform such as a microfluidic device [2, 13, 14]. Current in vitro cardiovascular tissue models incorporate cells from several sources to develop a functional integration of cardiomyocytes with capillary-like networks composed of endothelial cells. Human induced pluripotent stem cell (hiPSC) derived cardiovascular cells (cardiomyocytes, endothelial cells, and stromal cells) have been predominately used in cardiac organoid and tissue-on-a-chip models because of their potential to create patient-specific testing platforms for personalized medicine applications. Cardiomyocyte and endothelial cell differentiation methods have evolved from spontaneous embryoid body formation to directed differentiation of two-dimensional (2D) pluripotent stem cell monolayers with small molecules and growth factors. The latter methods modulate mechanistic pathways involving signaling via the Wnt, SMAD, and the MEK/MAPK to recapitulate developmental cardiogenesis and vasculogenesis during the differentiation and specification of cardiovascular cells in vitro [4, 6, 7, 9, 15-37]. Biomimetic extracellular matrix scaffold material used to develop 3D in vitro cardiovascular organoids must meet several requirements to ensure cell survival and function in addition to being safe and effective. First, the materials should be

biocompatible, so they support normal cellular function. The matrix should also be biodegradable so that it decomposes through inherent biological activities like hydrolysis or enzymatic degradation. The biomaterial should also have cell adhesion sites to promote cell attachment, migration, and paracrine signaling since the purpose of encapsulating cells in a scaffold is to improve their survival, retention, and function [6, 9, 10, 30-33]. Finally, the scaffold should be synthesized and cross-linked using mild and safe reagents. Scaffolds based on extracellular matrix (ECM) proteins, referred to as "natural" matrices, have dominated the field of cardiovascular tissue engineering due to their inherent biocompatibility and integrin binding sites that make them easier to use in complex in vitro or in vivo studies. The most commonly used protein biopolymers include collagen, gelatin, Matrigel, and fibrin [30, 31, 33, 34]. Hyaluronic Acid (HyA) and Alginate are the predominately used polysaccharide biopolymers for cardiovascular organoid ECM because they are biocompatible, biodegradable, non-immunogenic, and can absorb a large amount of water. HyA and Alginate do not have any cell binding motifs for cell attachment However, the biological and mechanical properties can be controlled through relatively easy chemical modification [30, 31, 33, 34]. Synthetic scaffolds commonly used in 3D cardiovascular tissue organoids include polyethylene glycol (PEG) and N-isopropyl acrylamide (NIPAAM) which provide stiffer ECM and temperature-dependent solidification properties [30, 31, 33, 34].

2. Outline

Below we summarize the primary approaches for building cardiac organoids as described in later sections. Our article focuses on these methods as they involve the adoption and use of disruptive technologies that can drive the field forward to high-throughput manufacture, testing, and evaluation of in vitro cardiovascular tissue models.

 Table 1. Approaches for bio-fabrication of cardiac organoids

Technique		Description	Important References
1.	Microfluidic technology- based platforms	Utilizes microfluidic devices such as biochips, also referred to as organ/tissue/lab-on-a-chip, to mimic microenvironments and processes that occur in human tissues. This technology provides controlled micro-environmental conditions including static and dynamic culture conditions, micro-surface topography, and surface-cell adhesion for studying 3D tissues and organoids.	[42-68]
2.	Micro- physiological systems (MPS)	Integrates a multicellular environment as well as mechanical factors such as stretching and perfusion, a 3D structure, and primary or stemcell-derived cells to mimic structural and functional similarity to human organs or tissues such as the myocardium.	[58-69]

3.	Microarrays and Microwell-based platforms	Implements the use of microwells in a poly (dimethylsiloxane) substrate to form consistent organoids with high uniformity and reproducibility. Multicellular aggregates enclosed in microwells are utilized as micro-scale organoids in different fields such as regenerative medicine and cancer biology.	[70]
4.	3D bio-printed models	This method follows the principle of additive manufacturing, which employs biomaterial scaffolds, cells, and growth factors to produce engineered constructs by utilizing complex 3D designs that resemble human tissues. 3D multicellular systems mimic the in vivo environment and are utilized to study developmental biology and diseases that occur in the human body.	[71-85]
5.	Electrospinning	Implements a relatively new technique to increase the biocompatibility of scaffolds utilized for cardiac applications. This technique fabricates nanofibers with adjustable structure, property, and functions utilizing various natural and synthetic biodegradable polymers. This is accomplished by using a charged polymer jet, which is deposited on a grounded collector. Deposition on fast-rotating collectors results in aligned nanofibers, while stationary collectors result in fiber mats that have no preferred orientation.	[86-107]

Other approaches that are not elaborated in this review include micropatterning, hydrogels, decellularization, and scaffold-free methods.

Micropatterning is the technique that utilizes a specialized photolithography microfabrication on a substrate by manipulating the preexistent surface or by adding a new layer of a previously constructed pattern, which facilitates the cells" proliferation and differentiation [38]. In one study, the authors developed an early cardiac organogenesis model in vitro using a protocol that combined biomaterials-based cell micropatterning with stem cell organoid engineering. As a result, 3D cardiac microchambers were created from hiPSC colonies, which resembled an early developing heart with distinct spatial organization and assembly [39].

Hydrogels made of water and a porous network of natural or synthetic polymers are widely implemented for fabricating tissue models or engineered heart tissues [40]. Hydrogels are solidified by the process of cross-linking, so that cells can be cultured on top of the hydrogel or interwoven (encapsulated) within the gel [41]. This technique is widely utilized due to the ease with which these materials replicate tissue characteristics such as stiffness and porosity, as well as allowing for cells" growth and communication

[42]. In one characteristic study, the team produced highly structured, heart-forming organoids (HFOs) by embedding human pluripotent stem cell aggregates in Matrigel followed by directed cardiac differentiation via biphasic WNT pathway modulation with small molecules. HFOs were found to be composed of a myocardial layer lined by endocardial-like cells and surrounded by a vascular network. The architecture of these HFOs closely resembles aspects of early native heart anlagen before heart tube formation, which is known to require an interplay with foregut endoderm development. These HFOs were applied to study genetic defects in vitro by demonstrating that NKX2.5-knockout HFOs show a phenotype reminiscent of cardiac malformations previously observed in transgenic mice [43].

Moreover, decellularization involves the process of utilizing an original tissue sample and using the native cells to produce a scaffold that resembles the extracellular matrix from the cells [38]. Decellularized ECMs have been employed as myocardial scaffolds, seeded with hiPSC-CMs and stromal cells to form cardiac patches [44], which then showed spontaneous contraction [45].

Likewise, scaffold-free methods utilize constructs such as cardiac spheroids. In a recently published study, the authors reported a self-assembly method to generate human heart organoids using human pluripotent stem cells. These heart organoids were produced through a three-step Wnt signaling modulation strategy using chemical inhibitors and growth factors and they matched human fetal cardiac tissues at the transcriptomic, structural, and cellular level. When developed further, they revealed internal chambers with well-organized multi-lineage cardiac cell types, with a complex vasculature, and exhibited robust functional activity [46]. Other shave also reported on self-assembling organoids from human pluripotent stem cells that have the ability to pattern and transform into chamber-like structures containing a cavity [47]. Cardiac cells derived and differentiated from human induced pluripotent stem cells play a distinct role in mature/adult cardiac functional recovery as adult cardiomyocytes are incapable of regeneration [48].

Human heart organoids can also be fabricated using different cell types, which are combined and result in heterogeneous tissue constructs that resemble different organ functions [49]. This method is highly efficient since biocompatibility is not an issue. Lastly, engineered heart tissue is an approach that utilizes cells found in the heart such as cardiomyocytes and matrix proteins, in combination, the cells form a bridge-like structure of tissue, which creates a 3D model that resembles tissue in vivo [50].

This manuscript conforms to the relevant ethical guidelines for human and animal research.

3. Engineering or Technology driven approaches for fabrication of cardiac organoids

3a. Microfluidic Tissue on a chip systems

Microfluidic technology has advanced different various areas of research by manipulating small volumes of fluids, broadening material selection, and fabrication

methods [51]. 2D studies have been used but are limited by their ability to accurately study biological and physiological characteristics that are affected by their cellular microenvironment. The size scale of the microchannels that can be fabricated in microfluidic devices is close to those of the microvascular system and these microchannel-based cell culture models can be used as perfusion cultures [52]. Microfluidics has expanded the ability to mimic microenvironments and processes that occur in native human tissues such as cellular activity and reactions by incorporating fluids that could be flowed, pumped, reserved, or separated within devices called tissueon-a-chip or lab-on-a-chip [51]. Micro-environmental conditions, such as static and dynamic flow, microsurface topography, and surface-cell adhesion can provide a platform for studying 3D tissues and organoids to reproduce functions in vitro to understand driving mechanisms for downstream actions, disease, and assessing toxicity [53]. Although cells are not cultured in a 3D matrix, their microenvironment can be designed to achieve this. Applying flow, cells, and a surface can show the difference in physiology and their response compared to static culture conditions and various flow rates [54]. Raasch et al. designed a biochip design for the culture of endothelial cell layers with improved perfusion conditions [55-57]. The biochip implemented perfusable membrane to aid cell culture by supplying medium, removing catabolic cell metabolites, and applying shear stress to endothelial cells (ECs) under controllable laminar flow conditions. Cell viability, expression of EC marker proteins and cell adhesion molecules of ECs dynamically cultured under low and high shear stress were compared to EC culture in 2D static conditions. Quantitative assays for cell viability and expression were simultaneously conducted by the static culture in order to compare the results to the dynamic platform. The results demonstrated that the ECs cultured with dynamic flow in the biochip were more representative of in vivo ECs than the other culture conditions in this study. In a study conducted by Sato et al. a microfluidic platform was developed to examine blood and lymphatic vessels for vascular permeability [52]. The microfluidic device consisted of an upper and lower channel that were partly aligned and separated by a porous membrane, where the blood vascular endothelial cells (BECs) and lymphatic endothelial cells (LECs) were co-cultured. Three different perfusion conditions were tested: static, pulsating flow, and continuous flow. Cell-viability and immunostaining for lymph-specific markers and transmembrane proteins were conducted on the cell cultures for 24 hours under static conditions in the microdevice. The live dead assay suggested the extent of cell death was below the detection limit. The immunofluorescence staining for VE-cadherin and claudin-5, the key components of endothelial adherens, were expressed at cell-cell junctions in both BECs and LECs. Permeability tests were conducted on the BEC-LEC bilayer cultured in the microdevice for 24 hours under a 1 μL/hour pulsating-flow condition, 1 μL/hour continuous-flow condition, and the static condition. All three conditions showed comparable levels of TRITC-dextran permeation, however, the LY-permeation level of the cells cultured in continuous and pulsating flow conditions was lower than the static culture cells. This suggests flow cultures promoted formation of endothelial cell-cell junctions. This study presented a model of BECs and LECs co-culture capable of

studying vascular permeability and lymphatic absorption studies. Kobuszewska et al. investigated the influence of static and perfusion conditions on cardiac cell proliferation, morphology, and alignment [58]. Three microdevices were designed with different microchamber geometries, a circular shape, a longitudinal microchannel shape, and three parallel microchannels separated by two rows of micropillars. Rat cardiomyoblasts (H9C2) cells were added to the H9C2 cell suspension and seeded into the culture chambers of each fabricated microdevice. The static culture consisted of placing H9C2 cells in a 96 well for 4-days in the incubator. For the microdevices subjected to static conditions, the cells were seeded and placed into the incubator for 24 hours to allow for cell adhesion and then placed in the incubator for 96 hours. For the perfused or dynamic condition, the cells were seeded into the culture microchamber at a flow rate of 5 μL/min and placed into the incubator for 24 hours, and every 24 hours following, the culture medium was replaced at a flow rate of 1 µL/min for 10 min until 96 hours were complete. The cell population changed over time in each of the three geometries following the first 24 hours for cell adhesion, although there was no significant difference. The cells in static cultures in the microdevices had a statistically significant increase in the number of H9C2 cells. H9C2 cell growth had the highest statistically significant increase in the microdevice with the longitudinal channel, followed by the circular chamber (128.6%), and lastly, the three parallel microchannels separated by two rows of micropillars (107%) after 48 hours. The exponential cell growth increase was dependent on the microdevice design. The circular microchamber microdevice experienced different flow rates within the microchamber, affecting H9C2 orientation. The microdevice with the longitudinal channel, the cells were elongated and strictly adhered to each other, mimicking the cell orientation in native myocardium tissue. In the microdevice with micropillars, the cells were mostly flattened and randomly oriented. The study concluded that the geometry of microdevices and micro environmental conditions (static and perfusion) influence H9C2 cell proliferation, morphology, and alignment.

Using a microfluidics-based approach our aim was to develop a high-throughput bioengineered human cardiac organoid platform, which provides functional contractile tissue with biological properties similar to native heart tissue, including mature, cell-cycle-arrested cardiomyocytes for drug development. Our group utilized a pillar/post-based design (~200 μm) adopted by others [59, 60], to assemble 3D cardiac organoids using a 3D Stereolithography (SLA) printed platform and cardiac cells including human AC16 CM, a proliferating cell line. All cells were homogenously mixed in a density of 1 \times 10 7 cells/ml within an alginate-gelatin bioink mixture using two luer lock syringes to make the cell density homogenous throughout the mixture. The cell-gel mixture was loaded into an SLA printed cassette with and without posts and the entire set-up was housed within a bioreactor at 10 rpm under standard culture conditions (37°C, 5% CO2) for 5 days. This optimized microfluidic device is expected to maintain continuous fluid circulation and laminar flow within the channels. The posts within the central chamber of the microfluidic device will serve as biophysical cues to help align cells in the cardiac

tissue to form organoids like self-assembled units and assist with continuously moving liquid through the device (unpublished observations). Furthermore, precise parameters such as fluid inlet velocities and viscocity, channel dimensions, effective mass transfer rates of nutrients and metabolic wastes, dynamic flow rates for matching the growth and remodeling of the organoids in relation to optimization of cell growth conditions was achieved by adoption of the Navier-Stokes equation.

Heart-on-a-Chip systems are developed by incorporating cardiac organoids into microfluidic chips/devices that facilitate fluid flow, gas exchange, biochemical signaling, and biophysical stimulus through the system. Microfluidic devices used with these models serve to maintain a controlled, sterile environment for the 3D tissue and move fluid through the system [2, 12, 15, 32, 35, 36, 61, 62]. Incorporating hiPSC-cardiovascular cells into relevant microfluidic devices provides a unique, patient-specific platform to study in vitro the complex process of CVD progression and the cellular response to biochemical and biophysical changes in their microenvironments [19, 63-66]. Recent studies have demonstrated functional cardiac, vascular, and multi-cellular cardiovascular organoids in microfluidic devices or platforms. The organoids within these systems self-assemble into structures that resemble human myocardium and provide physiologically relevant phenotype and gene expression output when exposed to external biochemical, biophysical, or environmental stressor stimuli [67-77].

Microphysiological systems (MPSs) go beyond the traditional 2D culture or monolayer cell assays by integrating several design characteristics such as multicellular environment, mechanical factors such as stretching and perfusion, a 3D structure, and primary or stem-cell derived cells. The addition of these characteristics increases the ability to create structural and functional similarity to human myocardium and vasculature composed of multiple cell types, incorporating cardiac conditions, monitoring different biomarkers for functional and morphological changes, and engineered materials for higher throughput models (**Figure 1**). MPSs can be designed and fabricated to facilitate reproducibility and support additional testing for tissue and organ development in vitro and drug discovery [78].

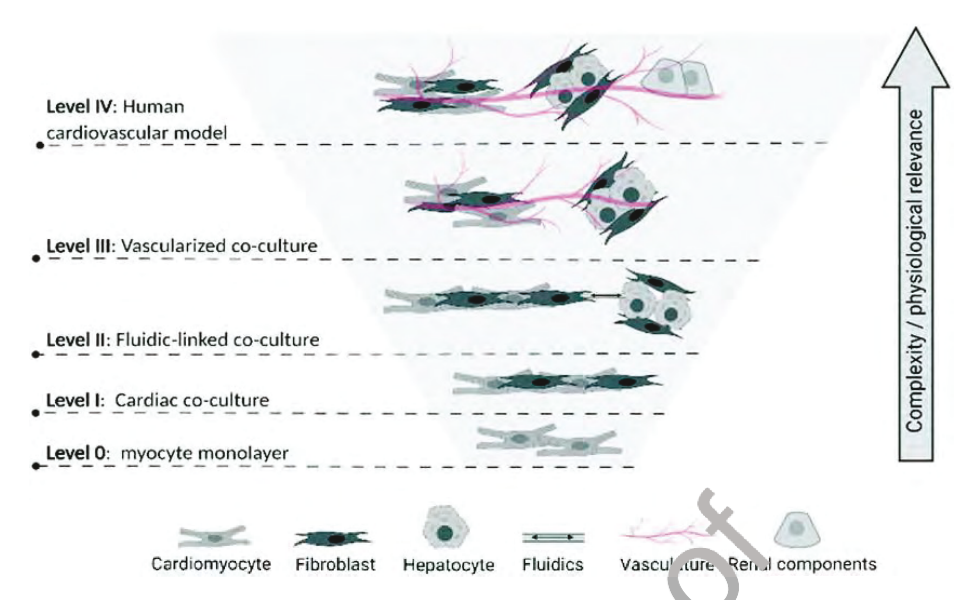


Figure 1. Proposed multi-tier categorization scheme of biological complexity levels for cardiovascular MPS models.

3b. 3D Multicellular aggregates and spheroids

Multicellular aggregation facilitated within microwells in a poly (dimethylsiloxane) (PDMS) substrate offers a promising solution for forming consistent organoids at high uniformity and reproducibility. These multicellular aggregates have been used as microscale organoids in the fields of, regenerative medicine, cancer biology and developmental biology for a long time. However, smaller aggregates (<1 mm corresponding to 500 cells per aggregate) pose a challenge for high throughput manufacturing and implementation. Albritton et. al custom-modified a commercial laser cutter to provide complete control over laser ablation to generate micro-wells (1800 micro wells per cm²) over large surface areas for multicellular aggregation (60 cm²). This approach enabled generation of micro-wells with a variety of sizes, contours, and aspect ratios. The study also demonstrated utility of these custom design laser ablated micro wells towards formation of multicellular aggregates using the following cell types, murine 344SQ metastatic adenocarcinoma cells, and human C4-2 prostate cancer cells that demonstrated epithelial lumen formation on Matrigel, and underwent epithelial to mesenchymal (EMT) and invasion in the presence of TGF-β. We adopted these custom designed micro wells (diameter-400 µm) for formation of multicellular aggregates or embryoid bodies using human mesenchymal stem cells (hMSCs). The PDMS micro well inserts were custom designed to fit 24-wells in standard well plates (ThermoFisher) and were coated with Pluronic F-127 solution using published procedures [79]. Approximately 5 X 10⁵ hMSC cells per well were seeded via pipetting using a multichannel micro-pipette. For even distribution of the cells, the micro well plate was gently rocked back and forth and sideways after which the plate was centrifuged in order to help force all cells into the microwells at 50xg for 2 minutes. The well plate was incubated at 37°C, 5% CO₂ for 48 hours to facilitate cell aggregation and growth. To harvest the multicellular aggregates, a fresh well plate was prepared by adding 2 ml of fresh media to the wells. The number of wells was kept constant to the number of micro well inserts that were used for cell aggregate harvest. Next, the micro well plate

containing cell aggregates was removed from the incubator and the spent media was removed. Following this, the PDMS plate was dislodged and transferred to fresh unused wells filled with media, in the multi well plate, using a pair of tweezers, it was ensured that the insert was inverted so that the micro wells were faced downward. The plates were centrifuged at 50xq for 2 minutes to force the formed cellular aggregates out of the micro wells into the newer wells. The formed hMSC cellular aggregates were collected and transferred to a conical flask using a micropipette and centrifuged to facilitate the formation of a pellet which was collected. This pellet was broken down and analyzed. Uniform sized clusters of human MSCs (~400 µm) formed after micro well culture for 48 hours in an incubator (Figure 2A). After retrieval from the micro wells these cell clusters retained viability as they adhered to the bottom of the well and started proliferating (Figure 2B). Cells cultured in non-Pluronic coated wells showed normal growth morphology (Figure 2C). Defined clusters of hMSCs formed after micro well culture for 48 hours in an incubator showed positive staining with Alkaline Phosphatase (ALP), indicating retention of pluripotency. Control human MSCs not coaxed to form clusters also retained pluripotency as shown by ALP staining (Figure 2D). This technique can be extrapolated to form cardiac organoids.

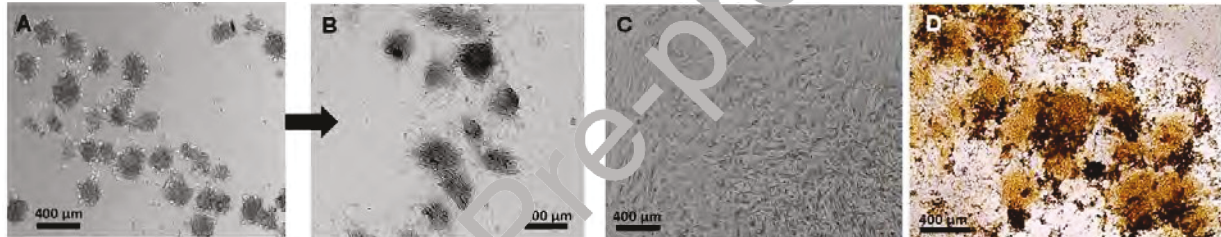


Figure 2. (A) Defined clusters of hMSCs formed in PDMS microwells coated with Pluronic after 48-hours of culture and incubation. (B) After retrieval these cell clusters retained viability as they depicted cell adhesion and growth. (C) HMSCs cultured in non-Pluronic coated wells depicted normal morphology. (D) The hMSCs clusters of formed after micro well culture for 48 hours in an incubator showed positive staining with ALP, indicating retention of pluripotency (unpublished data).

3D bioprinting uses a complex architectural design found in 3D tissues and translates it into a complex structure using additive manufacturing techniques that employs biomaterial scaffolds, cells, and growth factors to produce engineered constructs serving as physiological replicates of their in vivo counterparts. Different combinations of 3D bioprinting techniques and biomaterial scaffolds have been used for tissue engineering applications. 3D multicellular systems can be used to mimic the in vivo environment and also serve as promising alternatives to animal models to study cardiac developmental biology and recapitulate disease [80]. 3D spheroidal droplets are considered to be the most widely accepted models for 3D in vitro culture [81-83]. A scaffold with a spheroidal design is projected to offer an enhanced habitat for tissue formation as it enables sufficient distribution of oxygen, media, growth factors, nutrients, and ions into the scaffold for maintaining cell growth and proliferation. In prior published works, our laboratory has robustly demonstrated the potential of naturally derived hydrogels including gelatin, alginate, and collagen as naturally derived biodegradable materials for bioprinting of multilayered systems [84-90].

In a recently published study, we developed a cardiac organoid model using spheroidal droplets (<2 mm diameter) for facilitating the heterocellular coupling between cardiac myocytes (CM) and cardiac fibroblasts (CF) [91]. In the in vivo cardiac wall, CM and CF form extensive networks, with numerous physical contacts between these two cells and other supporting cells. The CF secrete the majority of the extracellular cardiac tissue matrix, and their number increases with aging and disease [92]. The CM form functional gap junctions with CF coupled by connexin-43 (Cx43) gap junctions which serves as a basis for electrical coupling of CM [93]. In our works, we have demonstrated proof of in vitro heterocellular coupling between CM and CF, facilitated by 3D bioprinting in vitro [86]. In a recent publication, we established a 3D cardiac tissue model that may facilitate the study of biomarkers for targeting therapeutic strategies to treat cardiac disease and thereby allow for a better understanding of cardiac biology. We expected that this 3D cardiac cell spheroidal droplet model would serve as a platform for enabling the heterocellular coupling between cardiac myocytes and fibroblasts for studying drug cytotoxicity effects in the future. After standardization of the 3D bioprinting parameters, this study resulted in high throughput production of 3D spheroidal droplets that exhibited interconnected porosity that promoted cell viability and function (Figure 3) [91].

In the setting of cardiac disease, enhanced cardiac myocyte and fibroblast heterocellular coupling may affect the electrical activity of the myocytes and contribute to arrhythmias. Thus, the heterocellular coupling phenomenon is key to understanding the potential active contribution of non-myocyte cells to cardiac electrophysiology and their relevance towards cardiac structure and function. In another recently published study [94], we developed 3D bioprinted scaffolds of hydrogel (gelatin-alginate) constructs encapsulated with a mixture of human cardiac AC16 cardiomyocytes (AC16-CMs), CFs, and microvascular ECs as cardiac organoid models in preparation for investigating the role of microgravity in cardiovascular disease initiation and development. We confirmed the heterocellular coupling normally exhibited between AC16-CM and CF by the expression of FSP-1 by the CF and CX43 by the CM. Due to the introduction of a third cell type, we expected all of the cells to communicate with each other through direct cell-cell interactions (CM-CF) and paracrine signaling (between EC and other cells), as both homotypic and heterotypic cell interactions contribute to the organized structure and proper function of the heart. We observed direct communication between all of the cells, CMs, CFs, and ECs, in the bioprinted scaffold, after 10-11 days of culture. The extent of the number of cell improved with time and was significantly greater at 10-11 days, which continued to increase, reaching a peak at 20-21 days, compared to earlier time points.

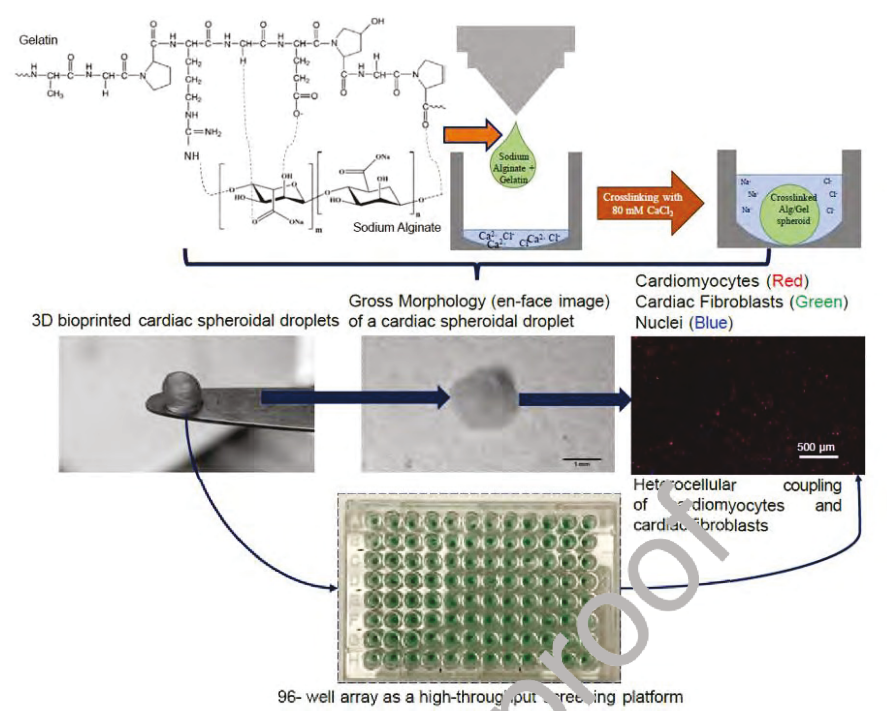


Figure 3. Outline and Schematic for cardiac spheroidal droplet formation. Reproduced from [91]. Copyright © 2021 Raven El Khoury et al. Exclusive Licensee Beijing Institute of Technology Press. Distributed under a Creative Commons Attribution License (CC BY 4.0).

3c. Electrospinning

Cardiac organoid engineering is aimed at creating in-vitro equivalents that can optimally duplicate the in-vivo functionality of human cardiac tissues. These organoid platforms are becoming valuable tools to model cardiac functions, for being used as preclinical platforms for drug testing, or alternatively be used as approaches for cardiac repair. Recent efforts in cardiac tissue engineering are being developed on enhancing the tissue regenerative ability of in-vitro cardiac tissue by targeting an increase in scaffold biocompatibility via the incorporation of various cell sources and bioactive molecules. Although primary cardiomyocytes can be successfully implanted via embedding within scaffolds, clinical translations of tissue engineering approaches are restricted. This is due to the lower cardiomyocyte survival rates and poor proliferation in traditionally designed hydrogel-based scaffolds owing to the lack of physical cues enabling cell adhesion, migration, and growth. New technologies must be introduced to improve myocardial regeneration to develop successful cardiac and cardiovascular tissue regeneration systems. Electrospinning is a simple, versatile technique for fabricating nanofibers with adjustable structure, property, and functions using various natural and synthetic biodegradable polymers that can be used for cardiac organoid fabrication. In this process, a charged polymer jet is deposited on a grounded collector, and a fast rotating collector results in aligned nanofibers while stationary collectors result in randomly oriented fiber mats [95]. Fiber dimension modification leading to changes in the nano-architecture of the scaffolds can increase cell survival, proliferation, and migration and provide supporting mechanical properties by mimicking micro-

environment structures, such as the ECM. In this section, we focus on the applications and types of electrospun nanofiber-based scaffolds for myocardial regeneration. We also highlight recent developments on stem cells and electrospun scaffolds combined to improve biocompatibility. We also describe the various aspects of fabrication of cardiac organoid constructs using electrospinning, from the choice of the components to their modeling, the final geometry of generated tissues, and the subsequent data and applications to model and treat cardiac diseases.

Naturally derived polymers possess non-toxicity of their degradation products and elicit an overall lower immune response making them ideal for in-vivo applications. The most commonly used natural polymers for electrospinning are collagen, alginate, chitosan, and gelatin. However, their application is challenged owing to their weak mechanical properties as a supportive scaffold and their rapid in-vivo degradation [96]. To overcome these disadvantages, naturally derived polymers have been electrospun in conjunction with other synthetic polymers to offer the flexibility of choice of biomaterials for tissue regeneration. The addition of synthetic polymers in electrospinning is beneficial because they can regulate the biodegradability of the resultant scaffolds biomaterials for longer periods and are minimally immunogenic. Moreover, they are highly economic and reproducible and have a simple quality control process.

Among synthetic polymers, polyglycolide (PGA), poly (L-lactide) (PLA), and poly (lactide-co-glycolide) (PLGA) have been widely used as clinical surgical sutures and implant materials due to their good mechanical properties and biocompatibility. PGA is known to exhibit the fastest rate of degradation followed by PGA > PLGA >> PGA. Furthermore, PLGA can be fabricated into nanofibers with larger diameters (760 nm) compared to PGA and PLA (-300 nm) [97]. Poly (ε-caprolactone) (PCL) is another biodegradable synthetic polymer that has been electrospun for a wide range of medical devices and implants. PCL is also known to exhibit a sustained degradation period, providing a sustained microstructure for prolonged therapeutic effects for tissue engineering applications [98]. A combinatorial approach using natural and synthetic polymer blend systems has been investigated to improve the materials and biological efficacy of electrospun scaffolds. The common goal of such electrospun polymer blend systems is to support increased cell adhesion, survival, growth, migration, and enhanced cell penetration within the core of the scaffolds [99]. In one study, electrospun fibers were made using a blend of PCL, poly (ethylene glycol) (PEG), and gelatin methacryloyl (GelMA). The blending of this hydrophobic-hydrophilic combination allowed for the preparation of a biomaterial that preserved the mechanical strength of PCL, while at the same time improving the hydrophilicity of the blended material and enhancing human osteoblast maturation [99].

Another approach to enhance biocompatibility is to modify the surface of the electrospun nanofibers to enhance cell adhesion and their drug loading ability. For example, PCL electrospun-fibers have been surface-grafted with gelatin to improve their compatibility with ECs for the enhancement of cell spreading and proliferation in vascular tissue engineering applications [100]. Other chemical modification methods

include surface-grafted modification by radiation, plasma, and chemical treatment for the formation of functional groups such as carboxyl, amine, hydroxyl-groups, and other hydrophilic or hydrophobic spacers [101].

Compared with one-component single nozzle electrospinning, blending of two or more components leads to the creation of electrospun fiber networks that may exhibit sustained biodegradability especially if the blend comprises a mixture of hydrophilic and hydrophobic polymers [102]. In a previously published study, Nagiah et. al made electrospun fiber mats using furfuryl-gelatin (f-gelatin), developed from visible light cross-linkable gelatin through the introduction of furfuryl groups [102] as summarized in Figure 4. Although these scaffolds had enhanced biocompatibility and surface topography as shown by scanning electron microscopy (SEM), mechanical testing performed on the aforementioned scaffolds showed an elastic modulus of 1.7 kPa. much lower than the expected values. So, the authors blended the hydrophilic f-gelatin with the hydrophobic PCL (50%:50%) to enhance the mechanical fidelity of the resultant scaffolds. We expected that combining PCL with f-gelatin would ensure that the hydrophobic PCL component would confer mechanical stability to the scaffold, while the f-gelatin would enhance biocompatibility to mimic the ECM properties of native cardiac tissue matrix. Next, we used a coaxial needle to electrospin scaffolds with PCL as the core and f-gelatin as the sheath to further enhance the structural stability of these blended scaffolds, as well as their biocompatibility. Uniform nanofibrous mats were produced in the scaffolds with a range of varying average fiber diameters of 760 ± 80 nm (f-gelatin only), 420 ± 110 nm [f-gelatin and PCL blended in 1:1], and 810 ± 60 nm (coaxial f-gelatin > PCL). Thermal analysis and Fourier transformed infrared (FTIR) spectroscopy revealed no interactions between the f-gelatin and PCL in the blended electrospun scaffolds. The difference in blending (single nozzle versus coaxial) methods led to significant differences in the elastic moduli of the electrospun scaffolds with the coaxial scaffolds demonstrating the highest elastic modulus of all scaffolds with an average elastic modulus of 164 ± 3.85 kPa. However, the biocompatibility of all scaffolds remained unaltered when evaluated with human AC16-CM cells and hiPSCderived CM, thereby demonstrating the potential of electrospun scaffolds for being adopted as platforms for cardiac organoid models.

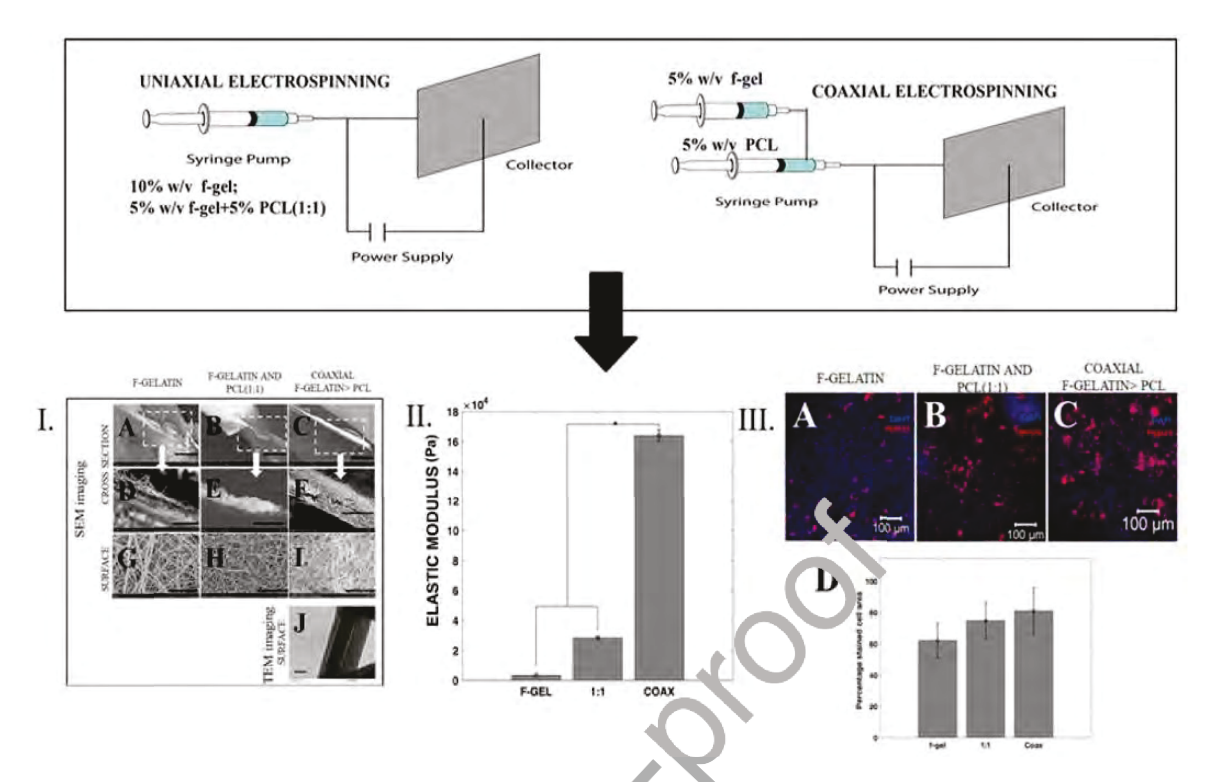


Figure 4. Outline and Schematic for single- and coaxial-electrospinning of f-gelatin blended with PCL to yield nano-fibrous scaffolds for cardiac tissue engineering applications. Reproduced with permission from [102].

Since the discovery of Vinyon N (nylon) by Voorhees and Dacron by DeBakey, the development of artificial vascular grafts was significantly advanced [103]. Although the transplantation of larger vascular grafts (with a diameter of > 6 mm) faced no challenges due to their prominent high-flow rate, the development of thrombi and increase of compliance mismatch have been shown in a small diameter vessel grafts [104]. To overcome these limitations, advanced techniques including electrospinning of tubular vessel grafts have been developed to increase construct potency, via chemical modifications on surfaces with different coating methods. Among these strategies, the delivery of growth factors from these scaffolds is of paramount importance for vessel regrowth and regeneration. The culture of ECs on different electrospun nanofibers has been previously studied by many groups. The materials that have been electrospun include Collagen Type I, PCL-Collagen blend, PGA and Chitosan-PCL using the following cell types including endothelial α-SMA positive cells [105], ECs [106] and human umbilical vein endothelial cell (HUVECs) [107]. All of these reports collectively emphasized the capability of the electrospinning method to fabricate natural and synthetic polymers fibers supplemented with various growth factors for cardiovascular tissue engineering.

A similar approach can be built via the incorporation of growth factors and other biomolecules to enhance stem cell adhesion onto electrospun scaffolds to improve their retention and survival leading to in vivo transplantation that is critical for regenerative

medicine. One study reported the cardiomyogenic differentiation of hMSC cells seeded on electrospun scaffolds made from a blend of PLA-PCL, gelatin and VEGF [108]. In another study, a cylodextrin/PEG-b-PCL-(dodecanedioic acid)-polycaprolactone-poly(ethylene glycol) (MPEG-PCL-MPEG) mixture was developed to reduce myocardial infarct expansion and to inhibit left ventricle (LV) re-modeling [109]. All of these studies confirmed improved cardiac function with no cell death.

Electrospinning with the encapsulation of biomolecules or drug-moieties results in fibers that may exhibit a more sustained release profile of these target molecules without an early burst release resulting from the physical adsorption technique [101]. These encapsulated bio- or drug-molecules can sustain their activity for a long-term release when released steadily from an electrospun scaffold. However, the electrospinning technique is often criticized due to the denaturation of the biomolecules resulting from conformational changes in the organic solvent environment. This drawback can be overcome by choosing the chemistry of the polymer backbone to effectively enable and regulate the degradation profile [110]. Toh et. al produced PLGA electrospun nanofibers combined with bFGF for tissue engineering applications [111]. The PLGA nanofibers containing bFGF efficiently discharged the protein for upto two weeks resulting in increased collagen production and an upregulation of gene expression of ECM-related proteins.

Electrospun scaffolds are valuable for cardiac regeneration as they provide an environment capable of providing the synchronized beating of cardiomyocytes and promote overall contractile function of the cardiac tissue as well as the anisotropic structure of the native myocardium in vivo. Based on such premise, one study reported an electrospun scaffold with elastomeric and biodegradable properties, and fabricated from poly(glycerol sebacate) (PGS): gelatin which facilitated neonatal rat cardiac cell attachment, proliferation, differentiation, and contractile function of the cardiomyocytes [112].

Recently our group developed three types of electrospun scaffolds, including furfuryl-gelatin (f-gelatin) alone, f-gelatin with polycaprolactone (PCL) in a 1:1 ratio, and coaxial f-gelatin (sheath) scaffolds with PCL (core) to serve as in-vitro platforms or engineered cardiac tissue models [102]. Our results demonstrate a simplistic approach to produce visible light cross-linkable, blended, biodegradable nanofibrous scaffolds for cardiac organoid applications [102].

Nanofibrous hydrogels that combine electrospun fibers with hydrogels can provide a porous and aqueous environment helping the cells to migrate and proliferate atop such hybrid scaffolds. One study reported the use of collagen-like synthetic self-assembling nanofiber hydrogels that supported the attachment, growth, and function of both neonatal rat CM and human embryonic stem-cell-derived CM for cardiac tissue engineering [112]. Thus, adoption of such hybrid 3D functional scaffold systems can be used to generate 3D heart tissue.

Electrospun scaffolds have been also adopted to serve as a biodegradable in-vivo patches placed to repair the infarcted heart with delivery of cardiomyocytes [113, 114]. Recently such bioengineered cardiac patches have been constructed with thermoplastic polymers, such as PGA, PLA, and PCL, with the goal of increasing their long-term elasticity and mechanical characteristics [115]. Boccaccini et. al developed biocompatible, biodegradable and elastic heart patches from PGS that lead to an overall reduction in the cardiac wall stress [116].

4. Characterization of organoid models

4a. Electrophysiology (EPHYS)

Cerebral/Brain Organoids and EPHYS: Lessons Learned

Advancements in organoid models for neural and cardiac tissue have established the feasibility for the use of such a model for improved drug toxicity screening, disease pathogenesis, and other environmental simulations. Their use, combined with microfluidic devices and three-dimensional cell culture, has only furthered the capabilities of these constructs in various applications by coming closer to mimicking the physiological responses of native tissues. Of these, cerebral organoid models have become the most widely studied due to easily identifiable electrical occurrences by which intercellular communication is carried out in neurons. Thus, giving rise to characterization via electrophysiological (EPHYS) techniques as a critical validation tool for use in any application.

Neuronal lipid membranes are composed of mechanosensitive protein-gated channels that allow for the inward and outward flow of Na+, Ca+, K+, and Cl- ions. The flux of which is mitigated by the presence of electrical potential in the cell membrane. In response to stimulation, neurons transmit electrical signals, known as action potentials, along the axon to allow for the influx or release of ions. Action potentials caused by neuronal firing can then be observed via EPHYS techniques. Monitoring the electrophysiological responses produced by organoids has proven to be a useful indicator of the presence of a healthy, functioning cellular network. Perhaps the most distinguishing feature of tissue-on-a-chip models is the culture of cells in a 3-D environment rather than 2-D. This array allows for enhanced cell-cell communications, thus improving cellular activity as model conditions approach those observed in vivo. By this method, it is possible to achieve an arrangement in which there exist neighboring cells in x, y, and z directions for any given cell. This multi-directional cellular communication is imperative to developing "normal functioning" networks [117]. In case of cerebral organoids, the gel must be conductive to achieve an acceptable formation of pathways in culture while also allowing promoting cellular adhesion [118]. To accomplish this, studies have developed gel formulas using a variety of conductive polymers and nanoparticles including gelatin and alginate with polypyrrole (PPy) [119], poly(3,4- ethylenedioxythiophene) (PEDOT) cultured with polystyrene sulfonate (PSS) [120], and collagen hydrogel microfibers infused with PPy nanoparticles [118]. The latter two of which both showed promising results in effectively transmitting electrical signals throughout the gel as well as promoting the differentiation of neurons. In completing this optimization step, an environment conducive to cellular growth and activity is created

while also supporting the transmission of electrophysiological signals through the gels. Successes and continual optimization of EPHYS characterization for neuronal models has incited a shift towards the use of such techniques in cardiac models. Like neurons, cardiac cells possess a negative resting membrane potential that changes due to the outward flow of K+ ions, which can be measured as electrical current [121]. Though resting and stimulated potentials vary slightly from neuronal cells, it is understood that the same EPHYS techniques and organoid optimization concepts can easily be translated to cardiac organoids.

Systems: Patch-Clamp, Microelectrode Arrays (MEA)

Previous electrophysiology work relies on a traditional whole-cell recording technique known as patch-clamp. In this process, a micropipette tip connected to a recording electrode is placed in contact with a targeted cell. Suction is applied to create a seal between the cell membrane and pipette tip, thus isolating the ion channels in that region. The cell is stimulated via induced current or pharmaceutical delivery and the ion response is recorded in terms of measured voltage across the cell membrane [122]. This provides valuable insight into the electrophysiological properties of cells in response to intentional manipulation. However, this technique allows only for the observation of an individual cell"s response while also imposing damage to the cell membrane. Consequently, this method is supplemented with calcium imaging to corroborate cell-cell communication within the network. In one study, which utilized human iPSC-CMs derived from patients with autosomal polycystic kidney disease to study the development of cardiovascular disease which is often associated with the disorder. Calcium imaging revealed decreased sarcoplasmic reticulum content in the diseased cell types along with decreased PKD1 gene types. Whole-cell patch clamp recording was then utilized to assess L-type calcium currents, baseline action potentials, and drug responsiveness of diseased cells in comparison to control cells, enabling researchers to demonstrate proof of concept for the utilization of patientspecific iPSC models for human diseases [123]. As can be seen, the use of calcium imaging and patch-clamp electrophysiology in parallel has proven to be an effective tool for identifying formations and relative function of cellular networks in organoid models. Still, the limitations imposed by this technique offer no insight into network function as a whole, which has led recent studies to shift toward the use of microelectrode arrays (MEA) for the characterization of organoid function.

MEAs are chips consisting of multiple microscopic electrodes which are used to collect extracellular EPHYS data from a wide number of cells in a population. This provides significantly more data compared to patch-clamp technique, which utilizes only a single electrode and measures activity from a single cell, thus creating a higher-throughput model for organoid network characterization. One study successfully recorded both the spontaneous and evoked response electrical activity of hiPSC-derived neurons plated on a biochip coated with PDLO for up to 3 months [124]. This approach demonstrates the use of such devices for long-term observation of networks of cell cultures by multisite data acquisition which could not have been obtained with traditional methods. Though early works focused on recording data from a 2D culture grown over the top of

multi electrode arrays, increasing potential in applications for organoid models has led to the combination of this technology with 3D cultures maintained in microfluidic devices. Advancements in technology have also made possible the fabrication of MEAs in various arrays designed for specific applications such as those embedded in well plates, probe, and mesh-types to be embedded throughout the organoid [124, 125]. One example is 3D human spinal cord organoids placed on MEA plates to monitor cellular response to chronic pain treatment, the results of which proved to be successful in validating the use of this model for similar applications [126]. The placement of the scaffold on the array, however, may result in observing on the cells in contact with electrodes resulting in limited data acquisition and understanding of the organoid function as a whole. Multi-planar EPHYS recording via probe or mesh-type MEAs provide an enhanced opportunity for monitoring cellular response throughout the organoid. An ongoing study aims to accomplish this by integrating a Neuropixel probe into a microfluidic device fabricated from UV-curing resin, iCell (GABA) neurons in a 9:1 alginate-matrigel hydrogel are then injected into the device along the probe shank where they are maintained for further experimentation. They are supplemented with complete maintenance medium (iCell Neural Base Medium 1, iCell Neural Supplement A) which flows through inlets on either side of the organoid chamber. In shifting towards cardiac models, one approach has developed a "cyborg organoid" in which a nanoelectronic mesh is cultured onto a 2D sheet of hiPSC-derived cardiac progenitor cells and human mesenchymal stem cells. The nanoelectronics naturally woven throughout the culture and reconfigure into a 3D spherical morphology. This allows for the observation of EPHYS patterns throughout cell maturation with minimal perturbations to the culture [125]. Evolutions in MEA technology, including the probe and mesh-type systems, allow for the integration of the MEA into the tissue rather than at the surface for more abundant data acquisition relevant to the scaffold as a whole and vastly expand the scope for the validation of organoid models via electrophysiology.

4b. RNA-Sequencing

Changes in global gene expression profiles due to processing via various methods for organoid formation can be accessed via RNA-sequencing (RNA-seq), a high throughput-sequencing assay that can provide an unbiased quantification of all expressed genes in the engineered cardiac tissue-on-a-chip platform and will also allow identification of the key cellular signaling pathways that are perturbed, in response to environmental stressors. Generalized linear models (GLMs) can be adopted to identify differentially expressed genes before and after exposure as shown by prior published works [127, 128]. This can be a useful tool to reveal cell damage pre- and post-exposure to environmental stressors.

Analysis of transcriptome dynamics will also allow identification of the key cellular signaling pathways that may be perturbed by long term culture of the cardiac organoids. We can also leverage this data to assess the impact of heterocellular culture on aging/senescence or trans-differentiation. For downstream functional analysis, Gene Ontology (GO) enrichment and Gene Set Enrichment Analysis (GSEA) analysis can be performed on the differentially expressed genes. One such differentially expressed gene is the YAP/TAZ1 component that plays an instructive, role in the regulation of

myocardial growth [129]. In our preliminary studies, we compared the gene expression profiles of CM-CF cultures exposed to acute hyperglycemic stress condition to CM-CF cultures from control condition (**Figure 5**). This comparison revealed widespread, transcriptome-wide changes in gene-expression programs of CM-CF cultures. Specifically in this case, culture conditions lead to significant perturbation of the genes involved in cardiovascular development pathway (**Figure 5A**). We uncovered differential expression of YAP1, a key component of YAP1/TAZ pathway and we detected the differential regulation in the gene expression of the YAP/TAZ1a well-established regulator of myocardial growth (**Figure 5B**).

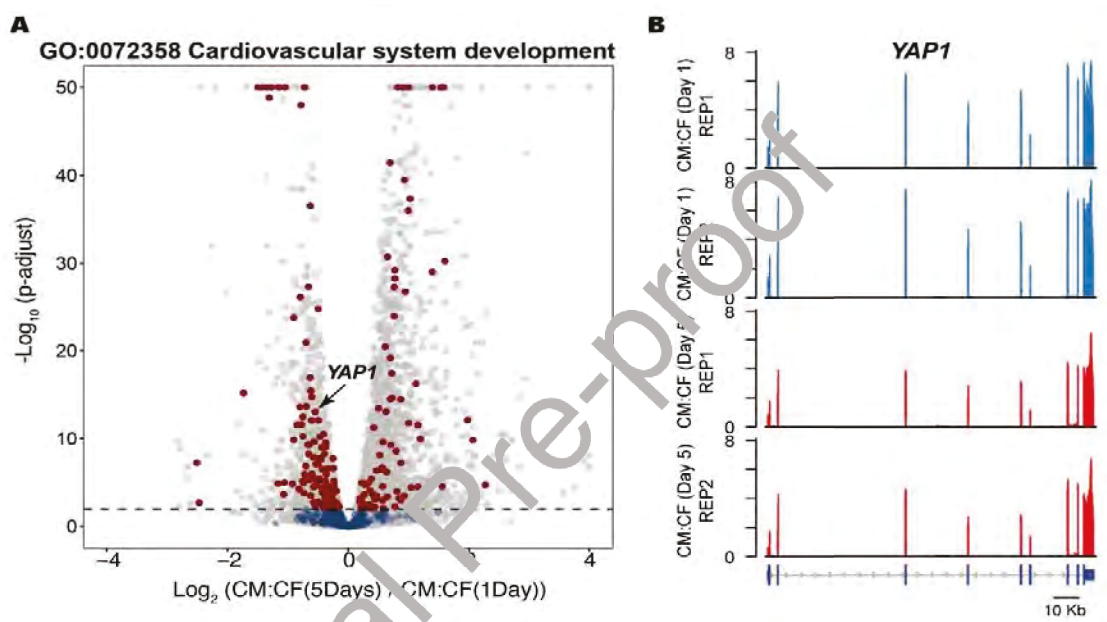


Figure 5. A) Cardiovascular system development pathway (GO ID: 0072358) was significantly perturbed in CM: CF cultures that were exposed to acute hyperglycemic stress conditions (5Days) in comparison to control (1Day). The red dots highlight the genes that are differentially expressed (Padjust<0.01) between the conditions. B) The change in gene expression profile of YAP1 (aligned reads normalized by total library size) (unpublished data).

Furthermore, advancements in next-generation sequencing (NGS) technologies have allowed for the study and characterization of individual cells. According to Hwang et al, single-cell RNA sequencing (scRNA-seq) provides an in-depth analysis of complex cell populations, cell lineages, as well as the relation between different genes [130]. This technique solves the limitations of bulk RNA-sequencing since scRNA-seq does not provide the average gene expression among multiple cells. ScRNA-seq allows scientists to obtain an unbiased analysis of cellular heterogeneity [131]. The implementation of these technologies has been critical in the development and implementation of 3D cardiac organoids. Additionally, scientists have developed a different range of single-cell methods to provide useful data. The workflow to perform scRNA-seq consists of sample preparation, single-cell capture, reverse transcription, amplification, library preparation, sequencing, and analysis [128].

For this technique, Differential Expression (DE) analysis and Gene Set Enrichment (GSE) analysis are most commonly used. DE identifies the different genes expressed in cell subpopulations as well as comparing gene expression between experimental conditions and case control samples, this analysis uses methods such as MAST, SCDE, and zingeR, which are used to analyze one gene at a time. Likewise, GSE provides the significant difference between two distinct biological states, this analysis utilizes multiple gene set analysis methods such as Significance Analysis of Function and Expression (SAFE) and Correlation Adjusted Mean RAnk (CAMERA) [132].

A single-cell approach is especially useful for cardiac applications due to the different cell types found in the heart. In previously published work scientists have implemented the use of RNA-sequencing to validate the mimicking characteristics of 3D cardiac organoids in relation to the human body [133-135]. Rossi et. al developed a multicellular cardiac organoid in which they implemented a scRNA-seq analysis, which resulted in gene expression sequences containing MESP1, RYR2, and alpha-actinin, which are markers of cardiac progenitor cells and mature cardiomyocytes. In addition, multiple studies have implemented 3D cardiac organoids for disease modeling. These studies implement scRNA-seq for testing the disturbance of genes involved in different cardiovascular diseases. Richards et. al utilized a cardiac organoid to model myocardial infarction and drug cardiotoxicity. The study compared the gene expression in control and infarct organoids by utilizing RNA-seq analysis. The resulting gene expressions were indicative of oxidative stress and heart contraction [136]. In summary, RNA-sequencing provides meaningful data that demonstrates whether an organoid resembles the biological characteristics of human tissue.

4c. Imaging and Algorithm based analysis

The development of 3D cardiac organoids and advanced imaging techniques to characterize these models necessitates a high-throughput, automated image analysis and quantification process [137]. Current image analysis algorithms are primarily written in Python or Matlab code and incorporate established computer vision libraries, packages, and modules (collectively called tools or algorithms) [138-142]. These tools like skimage-watershed and scipy-ndimage implement image analysis functions such as segmentation, sharpening, de-speckle, rotation/translation, and pixel intensity detection to identify and characterize objects of interest. The quantitative output of this analysis includes for these objects includes pixel intensity values (correlated to fluorescence intensity), automated counts per image, mean distance to nearest neighbor, and size/shape measurements. The basic workflow to incorporate ML image analysis in immunofluorescence organoid characterization is:1) staining 3D fluorescence/confocal microscopy to acquire z-stack images 3) organize/process Zstack images to desired quality with ImageJ or similar software, and 4) apply algorithm for automated image analysis [138-140].

Recent studies implementing machine learning (ML) image analysis of immunofluorescently stained organoids have demonstrated these algorithm-based approaches are reproducible, objective, and simple to use by inexperienced operators.

Gritti et. al [138] presented a Machine-learning-based Organoid Analysis software (MOrgAna), a Python program used to characterize morphological and fluorescence parameters for various samples. The sample types included human brain organoids, zebrafish explants (pescoids), mouse embryonic organoids (gastruloids), and intestinal organoids. Each sample type was maintained according to their respective culture procedures. All images were acquired in different conditions, such as microscopic devices, magnifications, and fields of view. Gastruloids were imaged every 24 h with the Opera Phenix High Content Screening System in wide-field mode with magnification and every 20 min for time-lapse. Pescoids were imaged on a benchtop Leica stereomicroscope S9i 11 h after pescoid generation. Brain organoids were imaged between 7 and 8 days on an Olympus FV3000 confocal microscope using a 10x objective with brightfield. To evaluate the segmentation of MOrgAna, a dataset of 91 organoid images were applied into CellProlifer and OrganoSeg. CellProlifer and OrganoSeg required processing, including smoothing, inverting image intensities, and removing debris by filtering objects. Three images were used to train the machine learning (ML) network for MOrgAna and directly applied to the remaining images in the dataset. The trained model was then used to predict unseen images. A custom Python script was used to perform a quantitative analysis to linearize the mask into a 1D array, compute the Jaccard distance, and output true positive (tp), true negative (tn), false positive (fp), and false negative (fn) pixel classification. The runtime was computed by manually monitoring the start and finish time for CellProfiler, OrganoSeg, and MOrgAna. When comparing runtime, CellProfiler processing time was more than twice as long compared to OrganoSeg and MOrgAna. When detecting global morphological changes in time lapse images, MOrgAna was capable of segmenting and quantifying small changes in brain organoids over time, including morphological shape, area, and perimeter. Fluorescent organoids were used to test the ability of MOrgAna to quantify and visualize elements, such as those in Gastruloids. Over the course of 5 days, MOrgAna presented an increase in brachyury expression over the course of 96 h of imaging. Time lapse images with 90 gastruloids and 144 time points were used to test the applicability of large datasets. Only ~1% of the total images were used to train the ML network and within a few hours, the entire dataset was analyzed resulting in ~0.5 TB of data and output graphs. MOrgAna displayed its ability to process hundreds of images, extracting morphological and fluorescence information, as well as, providing output graphs for the user. Additionally, MOrgAna can be used by new users with little to no image analysis or coding experience and experienced users, with the ability to customize code in the form of Jupyter notebooks and merged with the image analysis.

Toepfer et. al [139] developed a MATLAB software for large-scale analysis of sarcomere function in human induced pluripotent stem cell derived cardiomyocytes (hiPSC-CMs). This program, SarcTrack, was developed to monitor sarcomere count and dynamic changes in sarcomere length (SL), parameters for sarcomeres, percent and sarcomere contraction, relaxation durations, and cellular beat rate. These measures were obtained using fluorescent videos of labeled Z-disc or M-line pairs within each sarcomere. hiPSC-CM sarcomere proteins were fluorescently tagged using CRISPR/Cas9-mediated homology-directed repair of hiPSCs to introduce red

fluorescent protein (RFP) onto the carboxyl terminus of myomesin-1 (MYOM1-RFP), which is an M-band protein. For imaging, hiPSC-CMs were replated and imaged at day 30 after post-differentiation. Fluorescent tags were delivered by mApple-ACTN-2 lentivirus. Contractile forces were exerted by hiPSC-CMs on micropatterned fibronectin polyacrylamide hydrogel substrates at 1 Hz and videos of bead motion near the substrate surface were acquired at 30 frames per second. Five second video imaging on small hiPSC-CM clusters of 2 to 4 cells using a 100X objective of a fluorescent microscope at 30 frames per second. After removing sarcomeres of low fluorescence intensity, SarcTrack was able to detect real-time distances between sarcomere domains. To detect the duration of contraction and relaxation, individual sarcomeres were fitted to a period curve that could be custom designed. SarcTrack was compared to synthetic computer-generated sarcomeres. Here, Z-discs were generated with known parameters. Using two simulation contractions, SarcTrack was used to measure the synthetic sarcomeres and measured the prescribed values as identified. To assess contractility affected by fluorescent tags, SarcTrack analyzed GFP< RFP< and ACTN-2mApple, showing comparable contractility and relaxation durations. There was little variance across replicates for sarcomere shortening, resting SLs, contraction durations, and relaxation durations. Contractile parameters were quantified over differentiation days, showing trends such as sarcomere shortening increased at day 12 and reached a plateau by day 20. Contractile cycle parameters where quantified, revealing beat rate had a substantial impact on contractility parameters. In addition, parallel analyses with common cardiac drugs, such as Propranolol, showed effects on sarcomere performance while Verapamil, had minimal effects on duration of contraction and relaxation. SarcTrack demonstrated accuracy and functional assessment of sarcomeres in hiPSC-CMs. However, SarcTrack needed to account for fluorescent labeled, paired domains of sarcomeres in cells without high background signal. Input videos into SarcTrack must be 30 frames per second or more with good signal-to-noise ratio, which may limit the types of fluorescence confocal microscopes that cannot obtain high frame rate videos. SarcTrack demonstrated the ability to evaluate sarcomere contractile function with a set of 6 parameters and in turn fitted to an individual sarcomere in a frame, an application that can be used to address sarcomere analysis platforms.

Recently our groups conducted a cursory ML analysis on a small set of images collected during the course of our ongoing work developing cardiac organoids in dynamic microfluidic culture systems, presented in section 3a. This section describes a straightforward prototype image processing pipeline that is widely applicable to fluorescence-stained biomarker based images. We implemented customized image processing pipelines using computer vision techniques for approximating cell count, distribution, and stain absorption to quantify the extent of cardiac organoid formation in our studies. **Figure 6** shows representative images of our stained samples and automated image analysis written in Python code. Automated image analysis has been used to address most of these quantitative measurements [140]. The quantification process begins with preprocessing, where all z-stacked fluorescent images are scaled to the same magnification level, standardizing pixels per micron. Next, we converted

each image to grayscale and threshold using Otsu's method [141], for computing the Otsu threshold for each image and using the lowest observed threshold across the set as the standard. We eliminated noise from the thresholded images with an erosion operation, and then computed a distance transform map, which calculates the distance of each pixel to the nearest zero-valued pixel. The local peaks of the distance transformed images indicated the nominal centers of convex objects, and were used as seed points in a watershed segmentation [142]. The resulting segmentation yields instances of round image objects, corresponding to detected cells (Figure (6(a-b)) or clusters (Figure 6(c-d)) of cells. With cell clusters identified in comparison with no clusters, several quantitative metrics can be computed, including counts, densities, pixel brightness/intensity distributions, and cluster sizes. Shown in Figure 6(e) shows the main components of the Python code used in this automated image processing and Figure 6(f) is the resulting histogram with intensity profile for cell clusters observed under dynamic conditions with and without posts. Without the presence of posts, the cluster intensities are greater due to the homogenous spreading of cells throughout the culture platform.

In summary, a very simple processing pipeline can extract meaningful analytics for images of this type, enabling output of quantitative data. Notably, this processing pipeline requires no upfront manual annotation of images. While computer vision is more broadly approachable using deep learning techniques, this particular problem is better approached with conventional processing as there is no need for the large receptive field of a neural network, and the quantity of interest (intensity) is being measured directly. Future work will seek to standardize image capture and adapt algorithms appropriately to compare experimental variations.

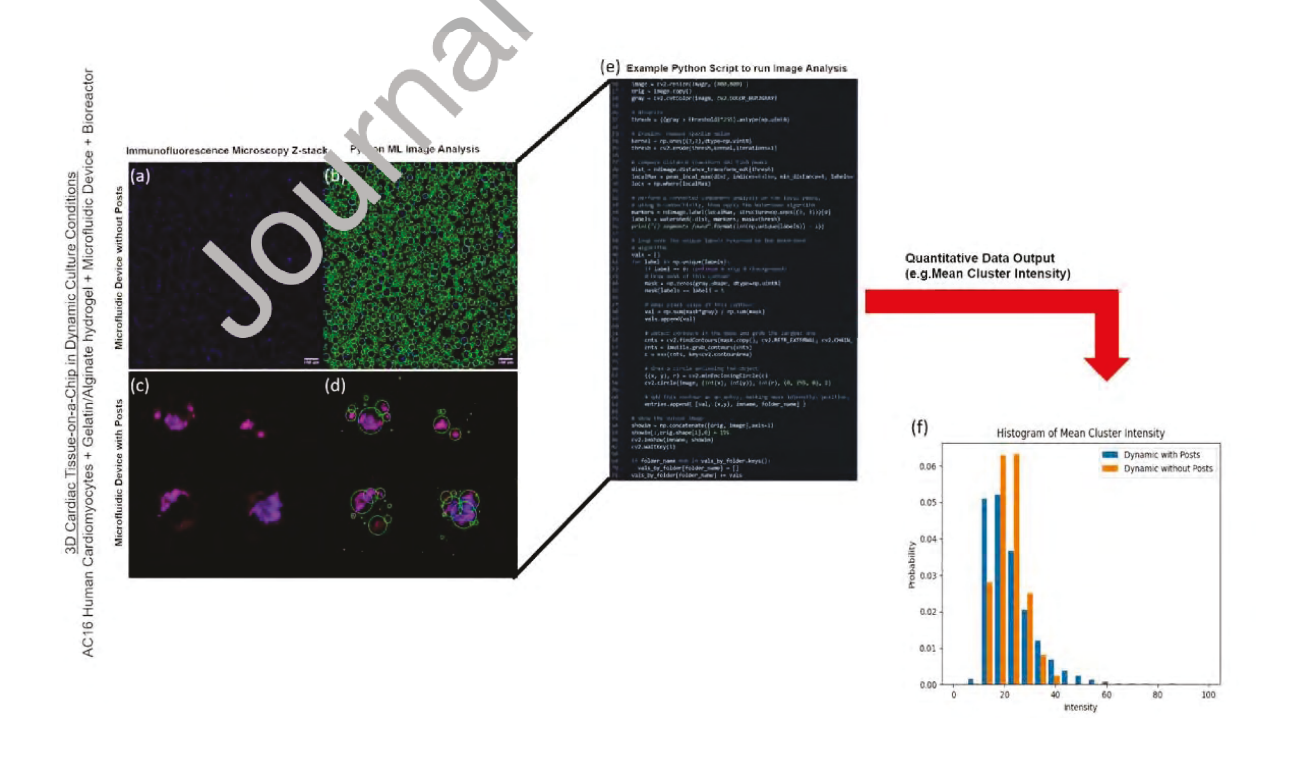


Figure 6. Representative images of our stained cardiac organoid samples and automated image analysis written in Python code. (a) Z-stacked image of f-actin (red) and dapi (blue) after 5-days of culture under dynamic conditions with no post. (Original image), (b) Processed image, showing minimum encompassing circles around detected clusters (c) Z-stacked image of f-actin (red) and dapi (blue) after 5-days of culture under dynamic conditions with posts. (Original image), (d) Processed image, showing minimum encompassing circles around detected clusters (e) main components of the Python code used in this automated image processing. (f) Histogram of cluster mean intensities for Dynamic with Posts vs. Dynamic without Posts images (unpublished data).

5. Discussion

Cell-cell and cell-ECM cues presented within 3D cardiac organoids allow the encapsulated cells to differentiate, migrate and self-organize thereby overcoming the limitations of 2D monolayer cultures [143]. Thus, the 3D organoid models bear the promise to transform and accelerate research on embryonic development, onset of diseases and drug development, thereby reducing the requirement for animal and in vivo models. Furthermore, using human iPSC derived cardiomyocytes key aspects of embryonic development of the heart can be studied, as well as our understanding of the genetic basis of development and pathophysiology of heart diseases can be probed. However, there are several limitations to 3D engineered cardiac organoid models as they require a high initial cell count for aggregation (3-6 \times 10⁶ cells/ml), within a complex equipment setup that may prevent high throughput screens [144]. In addition, drug cytotoxicity testing and disease modelling studies require the models to achieve maturation [145]. In order to facilitate long-term studies and to overcome maturation limitation of these 3D organoid models, development of these organoids via bioreactors is critical. Bioreactors facilitate biochemical signals by improving media circulation around the organoids to ensure higher uptake of physiological nutrients and removal of waste products [146]. In addition, the dynamic culture conditions induce shearing forces in bioreactor environment which has been shown to act as a mechanical stretching stimuli, promoting CM maturation [147]. Therefore, long-term bioreactor culture can lead to maturation of the organoids to match that of adult heart tissues.

The utilization of scaffolds and technology for scaling up the process of manufacturing 3D cardiac organoids is also vital in this regard. However, the success of these technologies e.g. 3D bioprinting, is largely dependent on the material properties, chemistry and crosslinking as well as shear thinning and viscosity of the ECM based bioink which remains variable across studies conducted by different groups in the field. However, precise control of cellular arrangement and spatial distribution of single cells can be accomplished via 3D bioprinting. Naturally derived or synthetically derived hydrogels and decellularized ECM have been developed into bioinks that serve as a scaffold for individual cell types for 3D bioprinting [87, 88, 91, 94]. Recently 3D bioprinting has been utilized to construct personalized cardiac patches matching the patient"s myocardium [148]. While these engineering approaches allow for highly controlled generation of cardiac constructs, they do not accurately capture developmental cues present for embryonic heart development and cannot recapitulate human cardiogenesis [149]. Biologically derived organoids driven by self-assembly on the other hand, exhibit self-organization and patterning properties and are thus of interest for studying these earlier developmental processes [150].

Owing to the rapid pace of advances in the technologies used for cardiac organoid development in recent years [16, 44-89, 94], a composite and scalable organoid model inspired by biology and driven by engineering and technology may soon be developed for studying of cardiac development and high-throughput disease modelling. **Figure 7** illustrates the steps that should be adopted to generate such a robust and physiologically relevant cardiac organoid model with multiple cardiovascular cell types followed by long-term maturation in a bioreactor system. Adapting these cardiac organoids for high throughput disease modelling will require assessment of cardiac function in real time, including electrophysiological measurements, contractile mechanical forces, and other physiological functions.

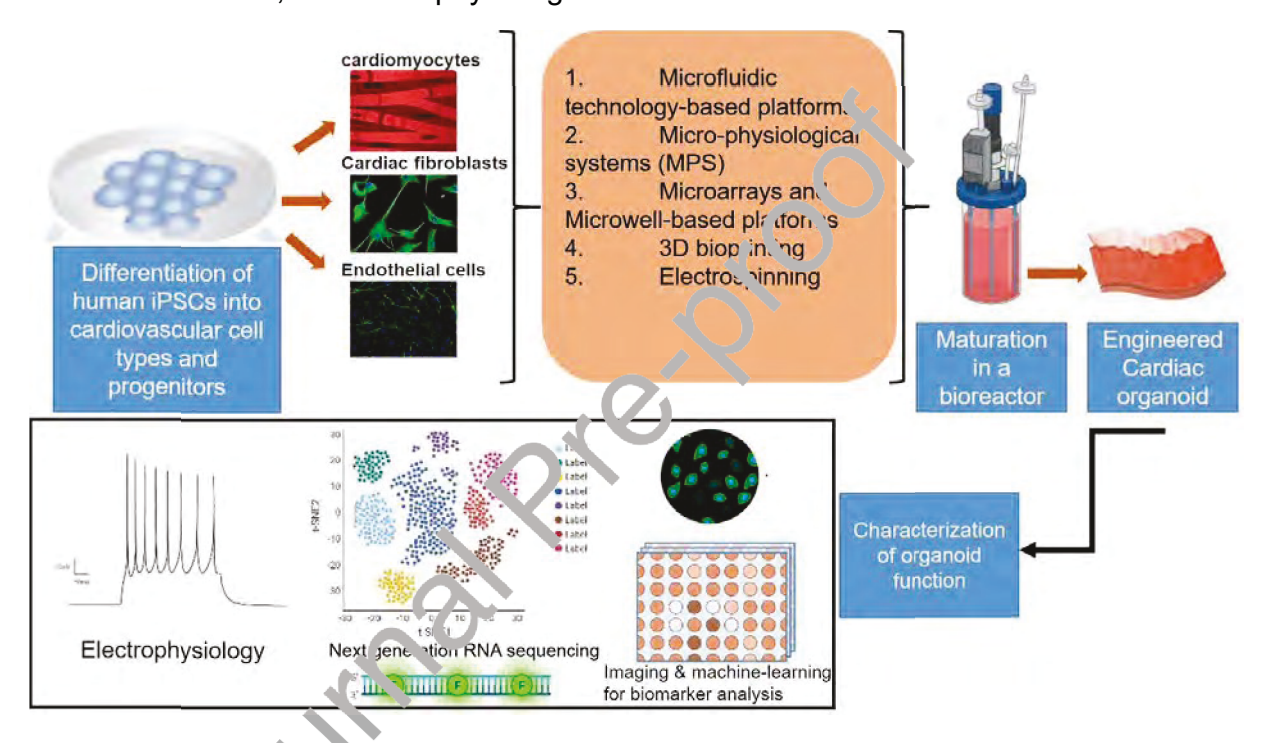


Figure 7. Schematic of the steps that can be adopted to generate robust and physiologically relevant cardiac organoid models with multiple cardiovascular cell types followed by long-term maturation in a bioreactor system

6. Conclusion

Future work for the cardiovascular organoid and heart-on-a-chip platform will target the development of more complex multicellular and multi-organ systems derived from a single-source such as human pluripotent stem cells to study specific biological reactions and diseases like cardiomyopathy, atrial fibrillation, myocardial infarction, and atherosclerosis. Additionally, more physiologically relevant cardiovascular tissue models will facilitate improved and accurate preclinical drug screening studies [2, 151-153]. The use of human induced pluripotent stem cells and incorporation of artificial intelligence/machine learning algorithms will allow patient-specific predictions of druginduced changes in human cardiac tissue and facilitate personalized medicine approaches [151, 154, 155].

Acknowledgements: Supported by the National Institutes of Health, NIH 1SC1HL154511-01 and the National Science Foundation, NSF 1927628 grants to BJ. SND acknowledges support from the University of Texas System Rising STARs Award. We also gratefully acknowledge help from Dr. Shweta AnilKumar, Dr. Jordan Miller, Dr. Irtisha Singh and Ms. Carla Loyola for technical expertise. All authors have reviewed the journal's policy on disclosure of potential conflicts of interest and have no conflicts of interest to declare. The authors have additionally reviewed the journal's authorship agreement and have all reviewed and approve the contents of this manuscript. The authors have no potential conflicts of interest to declare.

References:

- 1. Janssen, P.M., et al., *Preservation of contractile characteristics of human myocardium in multi-day cell culture.* Journal of molecular and cellular cardiology, 1999. **31**(8): p. 1419-1427.
- 2. Ronaldson-Bouchard, K. and G. Vunjak-Novakovic, *Organs-on-a-chip: a fast track for engineered human tissues in drug development.* Cell stem cell, 2018. **22**(3): p. 310-324.
- 3. Gimbrone Jr, M.A. and G. García-Cardeña, *Endothelial cell dysfunction and the pathobiology of atherosclerosis*. Circulation research, 2016. **118**(4): p. 620-636.
- 4. Lalit, P.A., et al., *Induced pluripotent stem cells for post—myocardial infarction repair: remarkable opportunities and challenges.* Circulation research, 2014. **114**(8): p. 1328-1345.
- 5. Mak, I.W.Y., N. Evaniew, and M. Ghert, Lost in translation: animal models and clinical trials in cancer treatment. American journal of translational research, 2014. **6**(2): p. 114.
- 6. Sanz-Nogues, C. and T. O'Brien, *In vitro models for assessing therapeutic angiogenesis.* Drug Discovery Today, 2016. **21**(9): p. 1495-1503.
- 7. Nsair, A. and W.R. MacLellan, *Induced pluripotent stem cells for regenerative cardiovascular therapies and biomedical discovery*. Advanced drug delivery reviews, 2011. **63**(4-5): p. 324-330.
- 8. Morin, K.T. and R.T. Tranquillo, *In vitro models of angiogenesis and vasculogenesis in fibrin gel.* Experimental cell research, 2013. **319**(16): p. 2409-2417.
- 9. Prestwich, G.D. and K.E. Healy, *Why regenerative medicine needs an extracellular matrix*. 2015, Taylor & Francis. p. 3-7.
- 10. Briquez, P.S., et al., *Design principles for therapeutic angiogenic materials*. Nature Reviews Materials, 2016. **1**(1): p. 1-15.
- 11. Wang, C., et al., *Maladaptive contractility of 3D human cardiac microtissues to mechanical nonuniformity*. Advanced healthcare materials, 2020. **9**(8): p. 1901373.
- 12. Veldhuizen, J., et al., *Engineering anisotropic human stem cell-derived three-dimensional cardiac tissue on-a-chip.* Biomaterials, 2020. **256**: p. 120195.
- 13. Ma, C., et al., *Organ-on-a-Chip: A New Paradigm for Drug Development.* Trends Pharmacol Sci, 2021. **42**(2): p. 119-133.
- 14. Andrysiak, K., J. Stępniewski, and J. Dulak, *Human-induced pluripotent stem cell-derived cardiomyocytes, 3D cardiac structures, and heart-on-a-chip as tools for drug research.* Pflugers Arch, 2021. **473**(7): p. 1061-1085.
- 15. Belair, D.G., et al., Human vascular tissue models formed from human induced pluripotent stem cell derived endothelial cells. Stem cell reviews and reports, 2015. **11**(3): p. 511-525.
- 16. Yoder, M.C., Differentiation of pluripotent stem cells into endothelial cells. Current opinion in hematology, 2015. **22**(3): p. 252.
- 17. Wilson, H.K., et al., *Concise review: Tissue-specific microvascular endothelial cells derived from human pluripotent stem cells.* Stem cells, 2014. **32**(12): p. 3037-3045.

- 18. Lian, X., et al., Robust cardiomyocyte differentiation from human pluripotent stem cells via temporal modulation of canonical Wnt signaling. Proceedings of the National Academy of Sciences, 2012. **109**(27): p. E1848-E1857.
- 19. Kusuma, S., et al., *Self-organized vascular networks from human pluripotent stem cells in a synthetic matrix.* Proc Natl Acad Sci U S A, 2013. **110**(31): p. 12601-6.
- 20. Bao, X., et al., Chemically-defined albumin-free differentiation of human pluripotent stem cells to endothelial progenitor cells. Stem cell research, 2015. **15**(1): p. 122-129.
- 21. Lian, X., et al., Efficient differentiation of human pluripotent stem cells to endothelial progenitors via small-molecule activation of WNT signaling. Stem cell reports, 2014. **3**(5): p. 804-816.
- 22. Harding, A., et al., *Highly efficient differentiation of endothelial cells from pluripotent stem cells requires the MAPK and the PI3K pathways.* Stem Cells, 2017. **35**(4): p. 909-919.
- 23. Prasain, N., et al., Differentiation of human pluripotent stem cells to cells similar to cord-blood endothelial colony–forming cells. Nature biotechnology, 2014. **32**(11): p. 1151-1157.
- 24. Adams, W.J., et al., Functional vascular endothelium derived from human induced pluripotent stem cells. Stem cell reports, 2013. 1(2): p. 105-113.
- 25. Youssef, A.A., et al., *The Promise and Challenge of Induced Pluripotent Stem Cells for Cardiovascular Applications.* JACC. Basic to translational science, 2016. **1**(6): p. 510-523.
- 26. Lee, S., et al., Enhanced therapeutic neovascularization by CD31-expressing cells and embryonic stem cell-derived endothelial cells engineered with chitosan hydrogel containing VEGF-releasing microtubes. Biomaterials, 2015. **63**: p. 158-167.
- 27. Marcelo, K.L., L.C. Goldie, and K.K. Hirschi, *Regulation of endothelial cell differentiation and specification*. Circulation research, 2013. **112**(9): p. 1272-1287.
- 28. Sommer, C.A. and G. Mostoslavsky, *Experimental approaches for the generation of induced pluripotent stem cells.* Stem Cell Research & Therapy, 2010. **1**(3): p. 1-7.
- 29. Zanotelli, M.R., et al., Stable engineered vascular networks from human induced pluripotent stem cell-derived endothelial cells cultured in synthetic hydrogels. Acta biomaterialia, 2016. **35**: p. 32-41.
- 30. Briquez, P., et al., *Design principles for therapeutic angiogenic materials.* Nature Reviews Materials, 2016. **1**: p. 15006.
- 31. Rice, J.J., et al., *Engineering the regenerative microenvironment with biomaterials*. Adv Healthc Mater, 2013. **2**(1): p. 57-71.
- 32. Jha, A.K., et al., Enhanced survival and engraftment of transplanted stem cells using growth factor sequestering hydrogels. Biomaterials, 2015. **47**: p. 1-12.
- 33. Lu, Y., et al., Bioresponsive materials. Nature Reviews Materials, 2016. 2(1): p. 16075.
- 34. Caliari, S.R. and J.A. Burdick, *A practical guide to hydrogels for cell culture*. Nat Methods, 2016. **13**(5): p. 405-14.
- 35. Natividad-Diaz, S.L., et al., *A combined hiPSC-derived endothelial cell and in vitro microfluidic platform for assessing biomaterial-based angiogenesis.* Biomaterials, 2019. **194**: p. 73-83.
- 36. Moya, M.L., et al., *In vitro perfused human capillary networks*. Tissue Eng Part C Methods, 2013. **19**(9): p. 730-7.
- 37. Belair, D.G., et al., *Human vascular tissue models formed from human induced pluripotent stem cell derived endothelial cells.* Stem Cell Rev Rep, 2015. **11**(3): p. 511-25.
- 38. Rogozinski, N., et al., *Current methods for fabricating 3D cardiac engineered constructs.* iScience, 2022. **25**(5): p. 104330.
- 39. Hoang, P., et al., Generation of spatial-patterned early-developing cardiac organoids using human pluripotent stem cells. Nat Protoc, 2018. **13**(4): p. 723-737.
- 40. Malda, J., et al., 25th anniversary article: Engineering hydrogels for biofabrication. Adv Mater, 2013. **25**(36): p. 5011-28.

- 41. Plotkin, M., et al., *The effect of matrix stiffness of injectable hydrogels on the preservation of cardiac function after a heart attack.* Biomaterials, 2014. **35**(5): p. 1429-38.
- 42. Caliari, S., et al., Stiffening hydrogels for investigating the dynamics of hepatic stellate cell mechanotransduction during myofibroblast activation. Scientific Reports, 2016. **6**: p. 21387.
- 43. Drakhlis, L., et al., *Human heart-forming organoids recapitulate early heart and foregut development.* Nature Biotechnology, 2021. **39**(6): p. 737-746.
- 44. Wang, Q., et al., Functional engineered human cardiac patches prepared from nature's platform improve heart function after acute myocardial infarction. Biomaterials, 2016. **105**: p. 52-65.
- 45. Guyette, J.P., et al., *Bioengineering Human Myocardium on Native Extracellular Matrix*. Circ Res, 2016. **118**(1): p. 56-72.
- 46. Lewis-Israeli, Y.R., et al., *Self-assembling human heart organoids for the modeling of cardiac development and congenital heart disease.* Nat Commun, 2021. **12**(1): p. 5142.
- 47. Hofbauer, P., et al., *Cardioids reveal self-organizing principles of human cardiogenesis*. Cell, 2021. **184**(12): p. 3299-3317.e22.
- 48. Voges, H.K., et al., *Development of a human cardiac organoid injury model reveals innate regenerative potential.* Development, 2017. **144**(6): p. 1118-1127.
- 49. Arai, K., et al., Fabrication of scaffold-free tubular cardiac constructs using a Bio-3D printer. PloS one, 2018. **13**(12): p. e0209162-e0209162.
- 50. Xiao, Y., et al., *Microfabricated perfusable cardiac biowire: a platform that mimics native cardiac bundle.* Lab Chip, 2014. **14**(5): p. 869-82.
- 51. Bahrami, S., et al., *Microfluidic devices in tissue engineering*, in *Biomedical Applications of Microfluidic Devices*. 2021, Elsevier. p. 209-233.
- 52. Sato, M., et al., *Microcirculation-on-a-chip: A microfluidic platform for assaying blood-and lymphatic-vessel permeability.* PloS one, 2015. **10**(9): p. e0137301.
- 53. Truskey, G.A., *Human microphysiological systems and organoids as in vitro models for toxicological studies.* Frontiers in public health, 2018. **6**: p. 185.
- 54. Zilberman-Rudenko, J., et al., *Utility of microfluidic devices to study the platelet–endothelium interface.* Platelets, 2017. **28**(5): p. 449-456.
- 55. Raasch, M., et al., *Microfluidically supported biochip design for culture of endothelial cell layers with improved perfusion conditions.* Biofabrication, 2015. **7**(1): p. 015013.
- 56. Lee, S., et al., *Microfluidic-based vascularized microphysiological systems*. Lab on a Chip, 2018. **18**(18): p. 2686-2709.
- 57. Cooper, M., J.L. Charest, and J. Coppeta, *Design principles for dynamic microphysiological systems*, in *Microfluidic Cell Culture Systems*. 2019, Elsevier. p. 1-29.
- 58. Kobuszewska, A., et al., *Heart-on-a-Chip: an investigation of the influence of static and perfusion conditions on cardiac (H9C2) cell proliferation, morphology, and alignment.* SLAS TECHNOLOGY: Translating Life Sciences Innovation, 2017.
- 59. Sticker, D., et al., *Multi-layered, membrane-integrated microfluidics based on replica molding of a thiol—ene epoxy thermoset for organ-on-a-chip applications.* Lab on a Chip, 2015. **15**(24): p. 4542-4554.
- 60. Olanrewaju, A., et al., *Capillary microfluidics in microchannels: from microfluidic networks to capillaric circuits.* Lab on a Chip, 2018. **18**(16): p. 2323-2347.
- 61. Huebsch, N., et al., Automated Video-Based Analysis of Contractility and Calcium Flux in Human-Induced Pluripotent Stem Cell-Derived Cardiomyocytes Cultured over Different Spatial Scales. Tissue Eng Part C Methods, 2015. **21**(5): p. 467-79.
- 62. Sharma, A., et al., *Multi-lineage Human iPSC-Derived Platforms for Disease Modeling and Drug Discovery.* Cell Stem Cell, 2020. **26**(3): p. 309-329.

- 63. Chung, A.S. and N. Ferrara, *Developmental and pathological angiogenesis*. Annu Rev Cell Dev Biol, 2011. **27**: p. 563-84.
- 64. Coulombe, K.L., et al., *Heart regeneration with engineered myocardial tissue.* Annu Rev Biomed Eng, 2014. **16**: p. 1-28.
- 65. Wilson, H.K., et al., *Concise review: tissue-specific microvascular endothelial cells derived from human pluripotent stem cells.* Stem cells (Dayton, Ohio), 2014. **32**(12): p. 3037-3045.
- 66. Yoder, M.C., *Differentiation of pluripotent stem cells into endothelial cells*. Curr Opin Hematol, 2015. **22**(3): p. 252-7.
- 67. Browne, S., S. Hossainy, and K. Healy, *Hyaluronic Acid Macromer Molecular Weight Dictates the Biophysical Properties and in Vitro Cellular Response to Semisynthetic Hydrogels.* ACS Biomaterials Science & Engineering, 2020. **6**(2): p. 1135-1143.
- 68. Charrez, B., et al., *Heart Muscle Microphysiological System for Cardiac Liability Prediction of Repurposed COVID-19 Therapeutics.* Front Pharmacol, 2021. **12**: p. 684252.
- 69. Lam, S.F., et al., *Microfluidic device to attain high spatial and temporal control of oxygen.* PloS one, 2018. **13**(12): p. e0209574-e0209574.
- 70. Weng, K.C., et al., *Human Induced Pluripotent Stem-Cardiac-Endothelial-Tumor-on-a-Chip to Assess Anticancer Efficacy and Cardiotoxicity.* Tissue Eng Part C Methods, 2020. **26**(1): p. 44-55.
- 71. Glaser, D.E., et al., *Organ-on-a-chip model of vascularized human bone marrow niches.* Biomaterials, 2022. **280**: p. 121245.
- 72. Sun, S., et al., *Progressive Myofibril Reorganization of Human Cardiomyocytes on a Dynamic Nanotopographic Substrate.* ACS Applied Materials & Interfaces, 2020. **12**(19): p. 21450-21462.
- 73. Hoang, P., et al., Engineering spatial-organized cardiac organoids for developmental toxicity testing. Stem Cell Reports, 2021. **16**(5): p. 1228-1244.
- 74. Sances, S., et al., *Human iPSC-Derived Endothelial Cells and Microengineered Organ-Chip Enhance Neuronal Development.* Stem Cell Reports, 2018. **10**(4): p. 1222-1236.
- 75. Browne, S., et al., *Stem cell-based vascularization of microphysiological systems*. Stem Cell Reports, 2021. **16**(9): p. 2058-2075.
- 76. Huebsch, N., et al., *Metabolically driven maturation of human-induced-pluripotent-stem-cell-derived cardiac microtissues on microfluidic chips.* Nature Biomedical Engineering, 2022. **6**(4): p. 372-388.
- 77. Lee-Montiel, F.T., et al., Integrated Isogenic Human Induced Pluripotent Stem Cell-Based Liver and Heart Microphysiological Systems Predict Unsafe Drug-Drug Interaction. Front Pharmacol, 2021. **12**: p. 667010.
- 78. Pointon, A., et al., *Cardiovascular microphysiological systems (CVMPS) for safety studies—a pharma perspective.* Lab on a Chip, 2021. **21**(3): p. 458-472.
- 79. Albritton, J.L., et al., *Ultrahigh-throughput generation and characterization of cellular aggregates in laser-ablated microwells of poly(dimethylsiloxane)*. RSC Advances, 2016. **6**(11): p. 8980-8991.
- 80. Au Sharma, P. and C. Au Gentile, *Cardiac Spheroids as in vitro Bioengineered Heart Tissues to Study Human Heart Pathophysiology.* JoVE, 2021(167): p. e61962.
- 81. Zuppinger, C., *3D cardiac cell culture: a critical review of current technologies and applications.* Frontiers in cardiovascular medicine, 2019. **6**: p. 87.
- 82. Pinto, B., et al., *Three-dimensional spheroids as in vitro preclinical models for cancer research.* Pharmaceutics, 2020. **12**(12): p. 1186.
- 83. Lazzari, G., P. Couvreur, and S. Mura, *Multicellular tumor spheroids: a relevant 3D model for the in vitro preclinical investigation of polymer nanomedicines.* Polymer Chemistry, 2017. **8**(34): p. 4947-4969.

- 84. Joddar, B., et al., *Development of functionalized multi-walled carbon-nanotube-based alginate hydrogels for enabling biomimetic technologies.* Scientific Reports, 2016. **6**: p. 32456.
- 85. AnilKumar, S., et al., *The applicability of furfuryl-gelatin as a novel bioink for tissue engineering applications*. Journal of Biomedical Materials Research Part B: Applied Biomaterials, 2018.
- 86. Anil Kumar, S., et al., A Visible Light-Cross-Linkable, Fibrin-Gelatin-Based Bioprinted Construct with Human Cardiomyocytes and Fibroblasts. ACS Biomaterials Science & Engineering, 2019. 5(9): p. 4551-4563.
- 87. Alonzo, M., et al., *Hydrogel scaffolds with elasticity-mimicking embryonic substrates promote cardiac cellular network formation*. Progress in biomaterials, 2020. **9**(3): p. 125-137.
- 88. Joddar, B., et al. *A 3D Bioprinted Human Cardiac Cell Platform to Model the Pathophysiology of Diabetes.* in *Circulation Research.* 2020. Am Heart Assoc.
- 89. Roman, B., et al., A Model for Studying the Biomechanical Effects of Varying Ratios of Collagen Types I and III on Cardiomyocytes. Cardiovascular Engineering and Technology, 2021.
- 90. Alonzo, M., El Khoury, R., Nagiah, N., Thakur, V., Chattopadhyay, M., Joddar, B., *3D Biofabrication of a cardiac tissue construct for sustained longevity and function.* . ACS Applied Materials & Interfaces., 2022.
- 91. El Khoury, R., et al., 3D Bioprinted Spheroidal Droplets for Engineering the Heterocellular Coupling between Cardiomyocytes and Cardiac Fibroblasts. Cyborg and Bionic Systems, 2021. **2021**.
- 92. Porter, K.E. and N.A. Turner, *Cardiac fibroblasts: at the heart of myocardial remodeling.* Pharmacology & therapeutics, 2009. **123**(2): p. 255-278.
- 93. Kohl, P., et al., *Electrical coupling of fibroblasts and myocytes: relevance for cardiac propagation.* Journal of electrocardiology, 2005. **38**(4): p. 45-50.
- 94. Alonzo, M., et al., 3D Biofabrication of a Cardiac Tissue Construct for Sustained Longevity and Function. ACS Applied Materials & Interfaces, 2022. **14**(19): p. 21800-21813.
- 95. Au Leach, M.K., et al., *Electrospinning Fundamentals: Optimizing Solution and Apparatus Parameters*. JoVE, 2011(47): p. e2494.
- 96. Venugopal, J.R., et al., *Biomaterial strategies for alleviation of myocardial infarction.* Journal of the Royal Society Interface, 2012. **9**(66): p. 1-19.
- 97. You, Y., et al., *In vitro degradation behavior of electrospun polyglycolide, polylactide, and poly (lactide-co-glycolide).* Journal of Applied Polymer Science, 2005. **95**(2): p. 193-200.
- 98. Sowmya, B., A.B. Hemavathi, and P.K. Panda, *Poly* (ε-caprolactone)-based electrospun nanofeatured substrate for tissue engineering applications: a review. Progress in biomaterials, 2021. **10**(2): p. 91-117.
- 99. Lobo, A.O., et al., *Electrospun nanofiber blend with improved mechanical and biological performance.* International journal of nanomedicine, 2018. **13**: p. 7891-7903.
- 100. Ma, Z., et al., Grafting of gelatin on electrospun poly (caprolactone) nanofibers to improve endothelial cell spreading and proliferation and to control cell orientation. Tissue engineering, 2005. **11**(7-8): p. 1149-1158.
- 101. Kim, P.-H. and J.-Y. Cho, *Myocardial tissue engineering using electrospun nanofiber composites.* BMB reports, 2016. **49**(1): p. 26-36.
- 102. Nagiah, N., et al., *Development and Characterization of Furfuryl-Gelatin Electrospun Scaffolds for Cardiac Tissue Engineering.* ACS Omega, 2022. **7**(16): p. 13894-13905.
- 103. Nosé, Y., *Dr. Michael E. DeBakey and His Contributions in the Field of Artificial Organs September 7, 1908–July 11, 2008.* 2008, Wiley Online Library. p. 661-666.
- 104. Stewart, S.F. and D.J. Lyman, *Effects of a vascular graft/natural artery compliance mismatch on pulsatile flow.* Journal of biomechanics, 1992. **25**(3): p. 297-310.

- 105. Weinberg, C.B. and E. Bell, *A blood vessel model constructed from collagen and cultured vascular cells.* Science, 1986. **231**(4736): p. 397-400.
- 106. Tillman, B.W., et al., *The in vivo stability of electrospun polycaprolactone-collagen scaffolds in vascular reconstruction.* Biomaterials, 2009. **30**(4): p. 583-588.
- 107. Du, F., et al., *Gradient nanofibrous chitosan/poly ε-caprolactone scaffolds as extracellular microenvironments for vascular tissue engineering.* Biomaterials, 2012. **33**(3): p. 762-770.
- 108. Tian, L., et al., Emulsion electrospun nanofibers as substrates for cardiomyogenic differentiation of mesenchymal stem cells. Journal of Materials Science: Materials in Medicine, 2013. **24**(11): p. 2577-2587.
- 109. Wang, T., et al., Bone marrow stem cells implantation with α -cyclodextrin/MPEG-PCL-MPEG hydrogel improves cardiac function after myocardial infarction. Acta biomaterialia, 2009. **5**(8): p. 2939-2944.
- 110. Liu, W., S. Thomopoulos, and Y. Xia, *Electrospun nanofibers for regenerative medicine*. Advanced healthcare materials, 2012. **1**(1): p. 10-25.
- 111. Sahoo, S., et al., *Growth factor delivery through electrospun nanofibers in scaffolds for tissue engineering applications.* Journal of Biomedical Materials Research Part A: An Official Journal of The Society for Biomaterials, The Japanese Society for Biomaterials, and The Australian Society for Biomaterials and the Korean Society for Biomaterials, 2010. **93**(4): p. 1539-1550.
- 112. Kharaziha, M., et al., *PGS: Gelatin nanofibrous scaffolds with tunable mechanical and structural properties for engineering cardiac tissues.* Biomaterials, 2013. **34**(27): p. 6355-6366.
- 113. Leor, J., et al., *Bioengineered cardiac grafts: a new approach to repair the infarcted myocardium?* Circulation, 2000. **102**(suppl 3): p. lii-56-lii-61.
- 114. Radisic, M., et al., Functional assembly of engineered myocardium by electrical stimulation of cardiac myocytes cultured on scaffolds. Proceedings of the National Academy of Sciences, 2004. **101**(52): p. 18129-18134.
- 115. Gao, J., P.M. Crapo, and Y. Wang, *Macroporous elastomeric scaffolds with extensive micropores* for soft tissue engineering. Tissue engineering, 2006. **12**(4): p. 917-925.
- 116. Chen, Q.-Z., et al., Characterisation of a soft elastomer poly (glycerol sebacate) designed to match the mechanical properties of myocardial tissue. Biomaterials, 2008. **29**(1): p. 47-57.
- 117. Osaki, T., V. Sivathanu, and R.D. Kamm, Engineered 3D vascular and neuronal networks in a microfluidic platform. Scientific reports, 2018. **8**(1): p. 1-13.
- 118. Wu, C., et al., *Cell-laden electroconductive hydrogel simulating nerve matrix to deliver electrical cues and promote neurogenesis.* ACS applied materials & interfaces, 2019. **11**(25): p. 22152-22163.
- 119. Ren, K., et al., Self-healing conductive hydrogels based on alginate, gelatin and polypyrrole serve as a repairable circuit and a mechanical sensor. Journal of Materials Chemistry B, 2019. **7**(37): p. 5704-5712.
- 120. Heo, D.N., et al., *Development of 3D printable conductive hydrogel with crystallized PEDOT: PSS for neural tissue engineering.* Materials Science and Engineering: C, 2019. **99**: p. 582-590.
- 121. Klabunde, R.E., *Cardiac electrophysiology: normal and ischemic ionic currents and the ECG.* Adv Physiol Educ, 2017. **41**(1): p. 29-37.
- 122. Neher, E. and B. Sakmann, *The patch clamp technique*. Scientific American, 1992. **266**(3): p. 44-51.
- 123. Lee, J.J., et al., Induced pluripotent stem cells derived from an autosomal dominant polycystic kidney disease patient carrying a PKD1 Q533X mutation. Stem Cell Res, 2017. **25**: p. 83-87.
- 124. Amin, H., et al., *Electrical responses and spontaneous activity of human iPS-derived neuronal networks characterized for 3-month culture with 4096-electrode arrays.* Frontiers in neuroscience, 2016. **10**: p. 121.

- 125. Li, Q., et al., *Cyborg organoids: implantation of nanoelectronics via organogenesis for tissue-wide electrophysiology.* Nano letters, 2019. **19**(8): p. 5781-5789.
- 126. Ao, Z., et al., *Human Spinal Organoid-on-a-Chip to Model Nociceptive Circuitry for Pain Therapeutics Discovery.* Analytical Chemistry, 2021.
- 127. Carrow, J.K., et al., *Widespread changes in transcriptome profile of human mesenchymal stem cells induced by two-dimensional nanosilicates.* Proceedings of the National Academy of Sciences, 2018. **115**(17): p. E3905-E3913.
- 128. Carrow, J.K., et al., *Photothermal modulation of human stem cells using light-responsive 2D nanomaterials.* Proceedings of the National Academy of Sciences, 2020. **117**(24): p. 13329-13338.
- 129. Artap, S., et al., *Endocardial Hippo signaling regulates myocardial growth and cardiogenesis.* Developmental biology, 2018. **440**(1): p. 22-30.
- 130. Hwang, B., J.H. Lee, and D. Bang, Single-cell RNA sequencing technologies and bioinformatics pipelines. Exp Mol Med, 2018. **50**(8): p. 1-14.
- 131. Paik, D.T., et al., Single-cell RNA sequencing in cardiovascular development, disease and medicine. Nat Rev Cardiol, 2020. **17**(8): p. 457-473.
- 132. Ma, Y., et al., Integrative differential expression and gene set enrichment analysis using summary statistics for scRNA-seq studies. Nat Commun, 2020. **11**(1): p. 1585.
- 133. Kerr, C.M., et al., *Multicellular Human Cardiac Organoids Transcriptomically Model Distinct Tissue-Level Features of Adult Myocardium.* Int J Mol Sci, 2021. **22**(16).
- 134. Mills, R.J., et al., Functional screening in human cardiac organoids reveals a metabolic mechanism for cardiomyocyte cell cycle arrest. Proc Natl Acad Sci U S A, 2017. **114**(40): p. E8372-e8381.
- 135. Rossi, G., et al., *Capturing Cardiogenesis in Gastruloids*. Cell Stem Cell, 2021. **28**(2): p. 230-240.e6.
- 136. Richards, D.J., et al., *Human cardiac organoids for the modelling of myocardial infarction and drug cardiotoxicity.* Nat Biomed Eng, 2020. **4**(4): p. 446-462.
- 137. Caicedo, J.C., et al., *Data-analysis strategies for image-based cell profiling.* Nat Methods, 2017. **14**(9): p. 849-863.
- 138. Gritti, N., et al., *MOrgAna*: accessible quantitative analysis of organoids with machine learning. Development, 2021. **148**(18).
- 139. Toepfer, C.N., et al., SarcTrack. Circ Res, 2019. 124(8): p. 1172-1183.
- 140. Strobel, H.A., et al., *Quantifying Vascular Density in Tissue Engineered Constructs Using Machine Learning.* Frontiers in Physiology, 2021. **12**(571).
- 141. Otsu, N., A threshold selection method from gray-level histograms. IEEE transactions on systems, man, and cybernetics, 1979. **9**(1): p. 62-66.
- 142. Vincent, L. and P. Soille, Watersheds in digital spaces: an efficient algorithm based on immersion simulations. IEEE Transactions on Pattern Analysis & Machine Intelligence, 1991. **13**(06): p. 583-598.
- 143. Langhans, S.A., *Three-Dimensional in Vitro Cell Culture Models in Drug Discovery and Drug Repositioning.* Front Pharmacol, 2018. **9**: p. 6.
- 144. Eder, A., et al., *Human engineered heart tissue as a model system for drug testing.* Adv Drug Deliv Rev, 2016. **96**: p. 214-24.
- 145. Turnbull, I.C., et al., Advancing functional engineered cardiac tissues toward a preclinical model of human myocardium. Faseb j, 2014. **28**(2): p. 644-54.
- 146. Van Winkle, A.P., I.D. Gates, and M.S. Kallos, *Mass transfer limitations in embryoid bodies during human embryonic stem cell differentiation*. Cells Tissues Organs, 2012. **196**(1): p. 34-47.

- 147. Phelan, M.A., P.I. Lelkes, and A. Swaroop, *Mini and customized low-cost bioreactors for optimized high-throughput generation of tissue organoids*, in *Stem Cell Investig*. 2018. p. 33.
- 148. Zhou, B. and W.T. Pu, *More than a cover: epicardium as a novel source of cardiac progenitor cells.* Regen Med, 2008. **3**(5): p. 633-5.
- 149. Pang, J.K.S., et al., *Insights to Heart Development and Cardiac Disease Models Using Pluripotent Stem Cell Derived 3D Organoids.* Front Cell Dev Biol, 2021. **9**: p. 788955.
- 150. Miyamoto, M., et al., *Heart organoids and tissue models for modeling development and disease.* Semin Cell Dev Biol, 2021. **118**: p. 119-128.
- 151. Chen, I.Y., E. Matsa, and J.C. Wu, *Induced pluripotent stem cells: at the heart of cardiovascular precision medicine.* Nat Rev Cardiol, 2016. **13**(6): p. 333-49.
- 152. Burnett, S.D., et al., *Cardiotoxicity Hazard and Risk Characterization of ToxCast Chemicals Using Human Induced Pluripotent Stem Cell-Derived Cardiomyocytes from Multiple Donors.* Chem Res Toxicol, 2021. **34**(9): p. 2110-2124.
- 153. Burnett, S.D., et al., *Human induced pluripotent stem cell (iPSC)-derived cardiomyocytes as an in vitro model in toxicology: strengths and weaknesses for hazard identification and risk characterization.* Expert Opin Drug Metab Toxicol, 2021. **17**(8): p. 887-902.
- 154. Lei, C.L., et al., *Tailoring Mathematical Models to Stem-Cell Derived Cardiomyocyte Lines Can Improve Predictions of Drug-Induced Changes to Their Electrophysiology.* Frontiers in physiology, 2017. **8**: p. 986-986.
- 155. Kowalczewski, A., et al., *Integrating nonlinear analysis and machine learning for human induced pluripotent stem cell-based drug cardiotoxicity testing.* J Tissue Eng Regen Med, 2022.